HHS Public Access

Author manuscript

Sci Immunol. Author manuscript; available in PMC 2021 September 08.

Published in final edited form as:

Sci Immunol. 2021 March 26; 6(57): . doi:10.1126/sciimmunol.abf0558.

A tumor-specific mechanism of T_{reg} enrichment mediated by the integrin αvβ8

Robert I. Seed[1,*], **Kenji Kobayashi**[1,*], **Saburo Ito**[1], **Naoki Takasaka**[1], **Anthony Cormier**[1], **Jillian M. Jespersen**[2], **Jean Publicover**[2], **Suprita Trilok**[2], **Alexis J. Combes**[1,3,4], **Nayvin W. Chew**[1,3,4], **Jocelyne Chapman**[5], **Matthew F. Krummel**[1,3], **Jianlong Lou**[6], **James Marks**[6], **Yifan Cheng**[7,8], **Jody L. Baron**[2,3], **Stephen L. Nishimura**[1,3,†]

[1]Department of Pathology, University of California, San Francisco, San Francisco, CA 94110, USA.

[2]Department of Medicine and Liver Center, University of California, San Francisco, San Francisco, CA 94143, USA.

[3]ImmunoX Initiative, University of California, San Francisco, San Francisco, CA 94143, USA.

[4]ImmunoX CoLabs, University of California San Francisco, San Francisco, CA 94143, USA.

[5]Department of Gynecology and Oncology, University of California, San Francisco San Francisco, CA 94110, USA.

[6]Department of Anesthesia and Perioperative Care, University of California, San Francisco, San Francisco, CA 94110, USA.

[7]Department of Biochemistry and Biophysics, University of California, San Francisco, San Francisco, CA 94158, USA.

[8]Howard Hughes Medical Institute, University of California, San Francisco, San Francisco, CA 94158, USA.

[†]Corresponding author. stephen.nishimura@ucsf.edu.

[*]These authors contributed equally to this work.

Author contributions: R.I.S., K.K., and S.L.N. established and developed the methodology and performed and analyzed in vivo and gene analysis experiments. A.C., A.J.C., S.I., J.L., J.M., and S.L.N. participated in antibody development, production, and characterization. Y.C., A.C., and S.I. participated in structural modeling. K.K., S.I., N.T., and S.L.N. participated in immunohistochemistry staining and analysis. R.I.S. and S.L.N. conceived and designed ex vivo lymphocyte cell culture assays. R.I.S., S.I., S.T., J.P., J.M.J., A.C., N.W.C., M.F.K., S.L.N., and J.L.B. performed flow cytometry experiments, RNAseq, and analysis. J.C. and S.L.N. performed human sample collection and processing. S.L.N. conceived, designed, and oversaw all experimentation. S.L.N., J.L.B., and R.I.S. wrote the manuscript. A.C. and N.W.C. provided biostatical support.

SUPPLEMENTARY MATERIALS

immunology.sciencemag.org/cgi/content/full/6/57/eabf0558/DC1

Materials and Methods

Fig. S1. β8 expression by tumor cells drives tumor growth, which is blocked by C6D4 Fab in vivo.

Fig. S2. Tumor T_{reg} isolation and expression of select T_{reg} genes by RNAseq in this report compared with single-cell RNAseq from splenic T_{reg}.

Fig. S3. Non-T_{reg} $CD4^+$ T cells express cell surface L–TGF-β, are converted to T_{reg} by contact with β8-LLC cells, and are the source of suppressive iT_{reg} generated on αvβ8.

Fig. S4. Murine nT_{regs} do not express detectable levels of cell-surface αvβ8.

Fig. S5. *LRRC32* (*GARP*) is most highly expressed by T_{reg} and stromal cells and *NRROS* by myeloid cells.

Table S1. Raw data table (Excel spreadsheet).

References (67–73)

View/request a protocol for this paper from Bio-protocol.

Abstract

Regulatory T cells (T_{regs}) that promote tumor immune evasion are enriched in certain tumors and correlate with poor prognosis. However, mechanisms for T_{reg} enrichment remain incompletely understood. We described a mechanism for T_{reg} enrichment in mouse and human tumors mediated by the αvβ8 integrin. Tumor cell αvβ8 bound to latent transforming growth factor–β (L–TGF-β) presented on the surface of T cells, resulting in TGF-β activation and immunosuppressive T_{reg} differentiation in vitro. In vivo, tumor cell αvβ8 expression correlated with T_{reg} enrichment, immunosuppressive T_{reg} gene expression, and increased tumor growth, which was reduced in mice by αvβ8 inhibition or T_{reg} depletion. Structural modeling and cell-based studies suggested a highly geometrically constrained complex forming between αvβ8-expressing tumor cells and L–TGF-β–expressing T cells, facilitating TGF-β activation, independent of release and diffusion, and providing limited access to TGF-β inhibitors. These findings suggest a highly localized tumor-specific mechanism for T_{reg} enrichment.

INTRODUCTION

Regulatory T cells (T_{regs}) are enriched in subsets of cancers and associated with poor clinical prognoses (1–3). T_{regs} suppress antitumor immune responses, with T_{reg} depletion promoting effector $CD8^+$ T cell immunity (4–6). Tumor-specific T_{reg} enrichment likely contributes to resistance to current immunotherapies (7). How T_{reg} enrichment occurs in tumors is not well understood, and a better understanding of this may improve antitumor therapies.

T_{regs} are induced by self-antigens in the thymus (tT_{regs}) or foreign antigens in extrathymic peripheral tissues (pT_{regs}) (8). tT_{regs} are recruited to tumors through chemokines specific to individual tumor types, whereas pT_{regs} are generated within tumors in response to signals generated within the tumor microenvironment (TME) (9, 10). The cytokine transforming growth factor–β (TGF-β) may contribute to pT_{reg} enrichment in tumors (11). TGF-β is critical for pT_{reg} generation because of its essential role in forkhead box P3 (FOXP3) expression during T_{reg} differentiation; the role of TGF-β in tT_{reg} generation is less clear (9, 12). Elucidating the role of TGF-β in pT_{reg} enrichment in tumors could help identify therapies specifically targeting the immunosuppressive effects of TGF-β while minimizing toxicities associated with systemic inhibition of TGF-β itself, TGF-β receptors (TGF-βRs), or T_{reg} depletion (6, 13–15).

TGF-β and its receptors are widely expressed in the TME (16, 17). TGF-β is always expressed in an inactive form within a latent complex, latent TGF-β (L–TGF-β), formed by noncovalent association of TGF-β with its prodomain, latency-associated protein (LAP) (18). On T_{regs}, TGF-β is presented at the cell surface through association with the scaffolding molecule glycoprotein A repetitions pre-dominant (GARP) (19). Within L–TGF-β, mature TGF-β cannot interact with its receptors unless undergoing “activation,” functionally defined as the acquired ability to initiate signaling through TGF-βRs.

TGF-β is cleaved intracellularly by furin from LAP, which has led to the widespread assumption that mature TGF-β must be physically released and diffused from the L–TGF-β

complex for activation and induction of signaling (20). However, why L–TGF-β needs to be presented on the cell surface by GARP if TGF-β diffusion gradients account for T_{reg} enrichment in tumors is unclear. L–TGF-β is present on the cell surface of $CD4^+$ T cells isolated from murine tumors (21), suggesting an alternative model where local regulation of TGF-β activation only on specific L–TGF-β–presenting $CD4^+$ T cells induces conversion to pT_{regs}.

The integrin αvβ8 may be an important mediator of tumor-specific regulation of TGF-β function (21). αvβ8 is highly expressed in multiple cancer types that have high numbers of T_{regs} (6, 21, 22). The LAPs of L–TGF-β1 and L–TGF-β3 contain arginine-glycine-aspartate integrin-binding sites, which are recognized by several integrins, particularly αvβ8, which is critical for TGF-β activation in immune cell function (23–26). L–TGF-β is the only physiologically relevant ligand for αvβ8, and thus, targeting αvβ8 selectively inhibits TGF-β function (27, 28). Anti-αvβ8 inhibits tumor growth of β8-expressing tumors, correlating with increased immune cell numbers and reversal of effector T cell exclusion; combination with anti–programmed cell death protein 1 (PD-1) improves these antitumor effects (21).

A structure-based model predicts that αvβ8 most efficiently activates L–TGF-β when αvβ8 expressed by one cell binds to cell-surface L–TGF-β presented by another. Within the cell-cell αvβ8/L–TGF-β complex, active TGF-β exclusively signals to the L–TGF-β–presenting cell because active TGF-β is not released and does not diffuse from the complex (29). Here, we found that a αvβ8/L–TGF-β complex formed between αvβ8-expressing tumor cells and L–TGF-β–presenting T cells was associated with T_{reg} enrichment in tumors. The αvβ8/L–TGF-β complex limited access to TGF-β inhibitors that would have otherwise been free to bind if active TGF-β was diffusible. These findings modify the conceptual framework for understanding how TGF-β functions in immune differentiation and affects therapeutic approaches to effectively and selectively inhibit it.

RESULTS

T_{regs} contributed to β8-dependent tumor growth

We investigated whether T_{regs} were required for protumorigenic effects of tumor cell αvβ8 using the syngeneic orthotopic β8-Lewis lung carcinoma (LLC) model (Fig. 1, A and B) (21). β8-LLC tumors had significantly more T_{regs} than non–β8-expressing mock-LLC tumors (Fig. 1, C and D). We depleted $CD25^+$ T cells with intraperitoneal injection of anti-CD25 (clone PC-61.5.3) 1 day after tumor implantation (30). PC-61.5.3 and anti-αvβ8 (clone C6D4) both reduced $FOXP3^+$ cells from β8-LLC tumors (Fig. 1, C and D). Neither antibody significantly affected $FOXP3^+$ cell numbers from mock-LLC tumors implanted on the contralateral side within the time frame in which euthanasia was required because of the size of the primary β8-LLC tumor (Fig. 1, C and D).

β8-LLC cells formed tumors significantly faster than mock-LLC tumors grown on opposite flanks, which was reduced by PC-61.5.3 or C6D4 (Fig. 1, E to M). PC-61.5.3 or C6D4 did not affect mock-LLC tumor volume or mass at day 14 after tumor cell injection (Fig. 1, E and G), consistent with the inability of PC-61.5.3 or C6D4 to reduce $FOXP3^+$ cells from mock-LLC tumors (Fig. 1, C and D). We confirmed the protumorigenic effects of tumor

cell αvβ8 in naturally β8-expressing TRAMP-C2 murine prostate carcinoma cells using a knockdown approach with *ITGB8* short hairpin RNA (shRNA) (fig. S1, A to H).

The mechanism of action of C6D4 could be from functional blockade of αvβ8-mediated TGF-β activation or effector function (i.e., antibody-dependent cellular cytotoxicity). To test the role of antibody effector function, we performed β8-LLC tumorigenicity assays using a Fab of C6D4 lacking the Fc region required for effector function (31). C6D4-Fab blocked β8-LLC tumor growth, similar to intact C6D4, compared with isotype control (fig. S1, I to L). These results demonstrated that C6D4 functions in the TME by blocking αvβ8 function, not by antibody effector function.

Tumor cell αvβ8 expression caused T_{reg} enrichment and an immunosuppressive T_{reg} transcriptome

PC-61.5.3 and C6D4 specifically reduced T_{reg} numbers and growth of β8-LLC but not mock-LLC tumors, suggesting that T_{regs} in β8-LLC tumors were distinct from T_{regs} in mock-LLC tumors. We hypothesized that αvβ8-expressing tumor cells participated in the local conversion of $CD25^+FOXP3^-$ T cells to $FOXP3^+$ pT_{reg}. The absence of an abscopal effect of T_{regs} generated in β8-LLC on contralateral mock-LLC tumor growth suggests that T_{regs} generated within αvβ8-expressing tumors are either retained or are phenotypically unstable outside the αvβ8-expressing TME because pT_{reg} may be less stable compared with tT_{reg} (32).

To test whether αvβ8-expressing tumor cells locally mediated conversion of $CD25^+FOXP3^-$ T cells to pT_{regs}, we determined the transcriptome of T_{regs} generated in β8-LLC compared with mock-LLC tumors. β8-LLC tumors had more T_{regs} than mock-LLC tumors, and anti-β8 reduced T_{reg} numbers in β8-LLC tumors, suggesting that tumor cell expression of αvβ8 correlated with $CD4^+CD25^+FOXP3^+$ T_{reg} enrichment (Fig. 2, B and C). We next performed RNA sequencing (RNAseq), evaluating the transcriptome of sorted T_{reg} pools from mock-LLC or β8-LLC tumors from mice treated with isotype (SV5) or C6D4 (Fig. 2, A, D, and E, and fig. S2A). Similarly high read counts for *FoxP3* and *Il2ra* (CD25) were seen in all T_{reg} pools, consistent with high T_{reg} purity (fig. S2B). Filtering of the dataset revealed 118 genes most highly and variably expressed across groups (Fig. 2, D and E).

T_{regs} from β8-LLC tumors had distinct transcriptional profiles that could be blocked by C6D4 to resemble T_{regs} from mock-LLC tumors. Comparison of T_{regs} from C6D4-treated β8-LLC tumors with T_{regs} from isotype-treated β8-LLC tumors revealed 116 of the 118 most variably expressed genes changed in the same direction ($R = 0.908$, $P < 0.0001$; Fig. 2D). Therefore, systemic blockade of αvβ8 with C6D4 had the same effect on the T_{reg} transcriptome as absence of β8 expression by tumor cells, demonstrating the importance of tumor cell αvβ8 to locally control T_{reg} gene expression. Hierarchal clustering of this gene set revealed tumor cell β8-dependent increases in expression of genes associated with T_{reg} immunosuppressive function and differentiation (i.e., *Il10*, *Ctla4*, and *Icos*; Fig. 2E) (6, 33). T_{regs} from β8-LLC tumors treated with isotype clustered separately from T_{regs} from C6D4-treated β8-LLC tumors or mock-LLC tumors (Fig. 2E). In contrast, T_{regs} from mock or β8-LLC tumors treated with C6D4 clustered together and were indistinguishable

(Fig. 2E). These data are consistent with the idea that tumor cell αvβ8 contributed to the enrichment of a T_{reg} population distinct from those infiltrating mock-LLC tumors.

The mechanisms underlying T_{reg} enrichment in tumors were likely to involve recruitment of T_{regs} and local T_{reg} conversion (2, 34). Recruited T_{regs} have increased representation of tT_{regs}, which potentially allows them to be distinguished from pT_{regs} by high expression of two markers, Helios (*Ikzf2*) and neuropilin 1 (*Nrp1*) (9, 34–38). However, both β8-LLC and mock-LLC tumor T_{regs} had low or un-detectable levels of *Ikzf2* and *Nrp1* in contrast to splenic T_{regs}, which consist of about 70% tT_{regs} and had high levels of these markers (fig. S2F) (36). Together, these data indicated that T_{regs} in β8-LLC tumors were skewed toward pT_{regs} rather than tT_{regs}.

L–TGF-β was expressed on the surface of T_{reg} and non-T_{reg} $CD4^+$ T cells

We next determined whether non-T_{reg} $CD4^+$ T cells expressed L–TGF-β on their cell surface and were therefore "primed" for T_{reg} conversion. There is cell surface expression of L–TGF-β on T_{regs} and activated non-T_{reg} $CD4^+$ T cells; however, no function has been attributed to this expression (19, 39, 40). Activated non-T_{reg} $CD4^+$ T cells [$CD4^+CD25^+GFP^-$ T cells from spleens of *FoxP3*-IRES-GFP mice (41)]] expressed increased cell surface L–TGF-β compared with nonactivated $CD4^+$ T cells (Fig. 3, A, B, and D, and fig. S3, A to H). Consistent with other reports, there were more L–TGF-$β^+$ cells in the $CD25^+FOXP3^+GFP^+$ T cell population (~8 to 22%) (Fig. 3, C and D). Thus, significant fractions of both non-T_{reg} $CD4^+$ T cells and T_{regs} express cell surface L–TGF-β. The physiological relevance of these findings is highlighted by the detection of L–TGF-β on the surface of both non-T_{reg} $CD4^+$ T cells and T_{regs} isolated from β8-LLC tumors (21).

Tumoral αvβ8 directly drove T_{reg} differentiation in vitro

We next tested whether binding of L–TGF-β on the surface of non-T_{reg} $CD4^+$ T cells to αvβ8 expressed on an opposing cell surface was sufficient to drive induced T_{reg} (iT_{reg}) conversion in vitro because iT_{regs} approximate many qualities of pT_{regs} generated in vivo (8). In this simplified system, iT_{reg} differentiation is mediated by binding to immobilized integrin αvβ8 independent of paracrine factors secreted by tumor cells, which could be influenced by αvβ8 ligand binding. The αvβ8 ectodomain is also free of cytoskeletal interactions, which modulate integrin conformational changes involved in force transduction and are important for TGF-β activation by the closely related integrin αvβ6 but not αvβ8 (23, 29, 42, 43). Culturing activated non-Treg $CD4^+$ T cells on immobilized αvβ8 (Fig. 3, E to G), but not αvβ3 [which does not mediate activation of TGF-β (Fig. 3, I to K) (29)], resulted in conversion to iT_{regs} as determined by increased FOXP3 expression and acquisition of suppressor function (fig. S3, I to L). T_{reg} conversion induced by αvβ8 was efficient (~60%) because it was similar to induction by a supraphysiologic concentration of recombinant TGF-β (rTGF-β; Fig. 3, F and O). Effects of αvβ8 on iT_{reg} differentiation were not due to ligation of L–TGF-β/GARP on activated T cells, or cell attachment, because no increase in iT_{reg} differentiation was seen when activated T cells expressing L–TGF-β were plated on wells coated with anti-LAP (fig. S3, M and N). Anti-β8 efficiently inhibited effects of immobilized αvβ8 on iT_{reg} differentiation (Fig. 3, G and H). αvβ8-mediated conversion to iT_{reg} depended on TGF-β, as demonstrated by blockade (~50%) with high

concentrations of a pan–TGF-β isoform antibody, 1D11 (fig. S3, V and W). The source of the active TGF-β mediating non-T_{reg} $CD4^+$ T cell conversion to T_{reg} on immobilized αvβ8 was not from secreted L–TGF-β in the media or from stimulated non-T_{reg} $CD4^+$ T cells (Fig. 3, Q and R). Last, αvβ8-mediated conversion to iT_{reg} required contact of non-T_{reg} $CD4^+$ T cells with αvβ8 (Fig. 3, S and T).

The immunosuppressive T_{reg} phenotype induced by immobilized αvβ8 was confirmed by significant β8-dependent induction of the immune checkpoint inhibitor *Ctla4* (Fig. 3L). *Ikzf2* and *nrp1* were barely or not detected, indicating that in vitro generated iT_{regs} were similar to the pT_{reg} phenotype seen in T_{regs} isolated from murine LLC tumors (Figs. 2 and 3L). In addition, low levels of *Ikzf2* and *nrp1* in αvβ8-generated iT_{regs} suggested that their origin was from non-T_{reg} $CD4^+$ T cells, not from the small (~1%) population of $CD25^+CD4^+FOXP3^+$ T cells mostly consisting of tT_{reg} (36). To directly address whether the iT_{reg} in our system originated from the non-T_{reg} $CD4^+$ T cell population, we sorted $CD4^+CD25^+GFP^-$ T cells, which were cultured on immobilized αvβ8 or αvβ3 as a control. Robust αvβ8-mediated conversion of $CD4^+CD25^+GFP^-$ to $CD4^+CD25^+GFP^+$ T cells was observed, demonstrating that the origin of iT_{reg} in our system was $CD4^+CD25^+$ GFP^- T cells and not expansion of the small population of $CD4^+CD25^+GFP^+$ T cells (fig. S3, Q to W). In contrast, sorted $CD4^+CD25^+GFP^+$ T cells from $CD4^+$ splenocytes displayed minimal expansion when cultured on immobilized integrins or in response to rTGF-β (fig. S3, R to T). These results indicated that iT_{regs} in our system originated from non-T_{reg} $CD4^+$ T cell populations rather than from expansion of existing T_{regs}.

To reproduce these results with αvβ8-expressing tumor cells, we cocultured activated non-T_{reg} $CD4^{+-}$T cells with β8-LLC cells and measured iT_{reg} conversion. Coculture with β8-LLC significantly increased iT_{reg} generation relative to mock-LLC cells (Fig. 3P and fig. S3, O and P). About 15 to 20% of non-T_{reg} $CD4^+$ T cells were converted to iT_{regs} in the presence of β8-LLC cells (Fig. 3P), similar to the efficiency of conversion to iT_{reg} on wells coated with αvβ8 at the same receptor density as β8-LLC cells (Fig. 5E). These results suggest that αvβ8 binding to L–TGF-β–presenting T cells, without any integrin cytoskeletal-mediated force transduction, was sufficient to mediate TGF-β activation and conversion of non-T_{reg} $CD4^+$ T cells to iT_{reg}, consistent with the integrin force-independent mechanism of TGF-β activation (29).

αvβ8 expression by nontumor cells was not essential for conversion of T cells to T_{reg}

We were unable to detect cell-surface αvβ8 on T_{regs} or conventional T cells (Tconvs) (fig. S4). These results mirror previous studies showing lack of αvβ8 expression on mouse $CD4^+$ and $CD8^+$ T cells, T_{regs}, macrophages, and dendritic cells (21, 29). However, it remains possible that levels of cell-surface αvβ8 on T cells or T_{regs} below the level of detection by cell surface staining are sufficient for T_{reg} generation and function (44, 45). However, we could find no evidence of significant *itgb8* gene or functional αvβ8 surface expression by T cells or T_{regs} in T_{reg} generation, function, or immunosuppressive gene expression either in vitro or in vivo [Figs. 1 (C to E and G to I), 2 (C to E), and 3 (I to K and H) and fig. S2 (D and G)].

ITGB8 was most highly expressed by tumor cells

We next sought to translate our αvβ8 cell-type expression data to the human TME by measuring the relative expression of *ITGB8* by various cell types in different human tumors. We performed bulk RNAseq of sorted immune (T cell, T_{reg}, or myeloid) and nonimmune (stromal or tumor) cells from human lung, gynecologic, and head and neck carcinomas (Fig. 4 and fig. S5, A to E). *ITGB8* was most highly and significantly expressed in tumor cells compared with immune cell populations in all three tumor types. *ITGB8* was also significantly expressed by stromal cells, albeit generally at a lower level than tumor cells. Rare samples with signal above background were seen in immune cells, likely representing technical noise, because such data points were identified as statistical outliers (Fig. 4, B to D). Accordingly, no significant expression of *ITGB8* was found in T_{regs} or other immune cell types known not to express *ITGB8*, such as $CD4^+$ T cells and myeloid cells (Fig. 4, B to D) (21). Together, our mouse and human findings support our conclusion that tumor cells are a functionally important site for αvβ8 expression in the TME.

L–TGF-β/GARP was most highly expressed by immune cells

Abundant evidence suggests that TGF-β expression by T cells, not tumor cells, is important to maintain an immunosuppressive TME (46–48). T cell surface localization of TGF-β may also be important in the TME because conditional deletion of *GARP* in T_{reg} inhibits growth of colitis-induced colon tumors (49). However, mechanisms of cell surface presentation of TGF-β in the TME have not been comprehensively studied. Thus, we next sought to determine which cells in the TME expressed TGF-β, *GARP*, or its functional homolog negative regulator of reactive oxygen species (*NRROS or LRRC33*) in the human TME.

TGFB1 was most highly and significantly expressed in $CD4^+$ T cells, with levels decreasing in rank order of T_{regs}, myeloid cells, and stromal and tumor cells (Fig. 4, E to G). *GARP* and *NRROS* were both expressed above background in different cell types; T_{regs} and stromal cells significantly expressed GARP, whereas myeloid, T_{reg}, and T cells significantly expressed *NRROS* (fig. S5). These data suggested multiple mechanisms for cell surface presentation of L–TGF-β; T_{regs} used both *GARP* and *NRROS*. Stromal cells used only GARP. Myeloid and T cells used *NRROS*, and tumor cells used neither (fig. S5). Our findings were consistent with previous identification of cell surface L–TGF-β on murine T cells, T_{reg}, and myeloid cells but not tumor cells from orthotopic tumors (21). Together, our data supported that $CD4^+$ T cells were a major source of cell surface L–TGF-β in the TME of human tumors.

Formation of a localized tumor/T cell αvβ8/L–TGF-β signaling complex

We next sought to test the physiological relevance of our structure-based model of TGF-β activation (Fig. 5A) (29) by asking whether αvβ8 expressed by tumor cell lines was sufficient to support TGF-β activation without release and diffusion of TGF-β from a cell-cell L–TGF-β/GARP complex. The respective αvβ8 cell surface receptor densities of β8-LLC (Fig. 5B), TRAMP-C2 (Fig. 5C), or human ovarian carcinoma (OVCAR-3; Fig. 5D) tumor cell lines were sufficient to efficiently support non-T_{reg} $CD4^+$ T cell–to–T_{reg} conversion (Fig. 5E). Accordingly, these β8-expressing lines efficiently increased TGF-β reporter activity in L–TGF-β/GARP– or L–TGF-β (R249A)/GARP–expressing transformed

mink lung cell (TMLC) reporter cell lines, with respective TGF-β activation efficiencies, correlating to αvβ8 surface receptor density (Fig. 5, E to H). These data demonstrated that αvβ8 expressed by tumor cells induced TGF-β signaling in L–TGF-β–presenting cells that they were in contact with.

Therapeutic implications of the tumor: T cell αvβ8/L–TGF-β complex

We developed a structural model of the αvβ8/L–TGF-β/GARP/TGF-βR2 signaling complex (29), which predicted numerous geometric constraints affecting binding of TGF-β protein inhibitors that have been developed to target freely diffusible mature TGF-β (Fig. 5A). Such inhibitors include antibodies to TGF-β, LAP, or GARP/L–TGF-β, as well as TGF-βR traps (29, 50–52). In contrast, the C6D4 antibody targets the αvβ8 ligand binding pocket and therefore would be predicted to efficiently prevent L–TGF-β binding to αvβ8 (29).

We used our TGF-β activation system to assess the relative ability of these inhibitors to block TGF-β activation. As predicted, anti-β8 (C6D4) efficiently inhibited TGF-β activation in wild-type (WT) L–TGF-β/GARP or L–TGF-β (R249A)/GARP reporter cells when plated on immobilized αvβ8, which, at low concentrations, was markedly more effective than antibody inhibitors to TGF-β, GARP, TGF-βR2, or TGF-βR2 receptor traps (Fig. 5, I and J). Decreased efficacy of antibody inhibitors to TGF-β, TGF-βR2, or TGF-βR2 receptor traps was due to the reduced ability to block mature TGF-β within the L–TGF-β complex because they were effective inhibitors of diffusible rTGF-β (Fig. 5K). These results were consistent with the inaccessibility of target epitopes for TGF-β, GARP, or TGF-βR2 within the αvβ8/L–TGF-β/GARP complex.

We next extended these findings to T cells themselves by using activated murine $CD4^+$ T cells plated on immobilized αvβ8 versus control substrates. T_{reg} generation on immobilized αvβ8 (Fig. 5L) was almost completely blocked by anti-β8 but was inhibited significantly less by other TGF-β protein inhibitors at the same concentration (Fig. 5, M to Q). The lack of efficacy of inhibitors preferentially targeting diffusible TGF-β supported our structure-based hypothesis that αvβ8-mediated T cell conversion to T_{reg} was independent of diffusion of TGF-β. This hypothesis was further tested using a Transwell filter assay (Fig. 5R), which demonstrated that non-T_{reg} $CD4^+$ T cells binding to αvβ8 induced iT_{reg} conversion only by non-T_{reg} $CD4^+$ T cells in direct contact and not those separated by the filter (Fig. 5, S to V). Together, our structural model of the αvβ8/L–TGF-β/GARP/TGF-βR2 signaling complex and comparative efficacy studies demonstrated a mechanism for T_{reg} enrichment dependent on αvβ8-mediated TGF-β activation.

β8 expression in non–small cell lung cancer positively correlated with T_{reg} density in the TME

Most of human cancers express αvβ8 in at least a fraction of tumor cells (21). We sought to test the hypothesis that a subpopulation of β8-expressing tumor cells was sufficient to drive local immunosuppressive T_{reg} differentiation. We correlated $CD4^+FOXP3^+$ cell numbers with β8 tumor proportion scores (TPS), which estimates the percentage of tumor cells expressing β8, in a cohort of non–small cell lung cancers (NSCLCs) distinct from the cohort used for RNAseq (Figs. 4 and 6). We assessed cells with dual staining

of CD4 and FOXP3 because most of these cells are T_{regs} (53). We found significant increases in $CD4^+FOXP3^+$ cell numbers with β8-TPS and $CD4^+FOXP3^+$ cell numbers and $CD4^+FOXP3^+$:$CD4^+FOXP3^-$ cell ratios correlated significantly with β8-TPS (Fig. 6, A to F).

To test the hypothesis that a limited proportion of β8-expressing tumor cells were sufficient to drive local T_{reg} differentiation, β8-expressing LLC cells with mock-LLC cells were mixed in varying proportions. A significant trend for enrichment of $FOXP3^+$ cells with increasing proportions of β8-expressing tumor cells was found (Fig. 6, G to J). Tumor growth correlated with $FOXP3^+$ cell proportions, consistent with T_{regs} contributing to β8-mediated tumor immune evasion (Fig. 6J). These results suggested that expression of αvβ8 in a small fraction of tumor cells was sufficient to drive T_{reg} enrichment in human tumors.

DISCUSSION

Here, we identified a mechanism of T_{reg} enrichment in tumors, where αvβ8 expression on tumor cells caused T_{reg} enrichment by increasing TGF-β activation in the TME. Our in vitro data suggested that the T_{reg} enrichment in β8-expressing tumors occurred via contact of αvβ8-expressing tumor cells with L–TGF-β–presenting non-T_{reg} $CD4^+$ T cells, converting them to pT_{reg}. We used cell-based assays to provide evidence that an intermolecular complex forms between αvβ8-expressing tumor cells and L–TGF-β–presenting non-T_{reg} $CD4^+$ T cell, where TGF-β was activated without release and diffusion of TGF-β and signaling was induced only on the L–TGF-β–presenting non-T_{reg} $CD4^+$ T cell.

Existing evidence supports two mechanisms of tumor T_{reg} enrichment, either intratumoral non-T_{reg} $CD4^+$ T cell conversion to pT_{reg} or recruitment of preexisting tT_{reg} to tumors (Fig. 7, A and B) (22, 24). While exogenous TGF-β can lead to conversion of T cells to iT_{regs}, no previous studies have addressed how TGF-β is activated in the TME or whether this activation leads to conversion of T cells to pT_{regs}, as seen in the murine colon (54). However, in human tumors, the relative importance of conversion of non-T_{reg} $CD4^+$ T cells to pT_{reg} is controversial because only a fraction of tumor T_{reg} share common T cell receptor (TCR) clonotypes with non-T_{reg} $CD4^+$ T cells (55, 56). Our analysis of human tumors does not allow discrimination of tT_{reg} from pT_{reg}; thus, it is unclear whether tumors with high αvβ8 expression have increased overlap between the TCR repertoires of non-T_{reg} $CD4^+$ T cells and T_{regs} compared with those from tumors with low αvβ8 expression.

Our study suggests that pT_{reg} enriched in murine αvβ8-expressing tumors contributed to tumor immune evasion because both PC-61.5.3 and C6D4 reduced T_{regs} in β8-LLC. PC-61.5.3 depletes intratumoral $CD4^+CD25^{hi}$ T cells when given after tumor cell injection but not $CD4^+CD25^{lo}FoxP3^+$ T cells (5, 30). Depleting T_{reg} precursors (L–TGF-$\beta^+CD4^+CD25^{hi}FoxP3^-$) in β8-LLC tumors would be expected to have the same effect as blocking αvβ8 function on intratumoral conversion to pT_{regs}. The mock-LLC T_{reg} population likely consists of $CD4^+CD25^{lo}FoxP3^+$ T cells because PC-61.5.3 failed to deplete it. Reducing T_{reg} by PC-61.5.3 or C6D4 decreased β8-LLC tumor growth, suggesting the importance of T_{reg}-induced immunosuppression in αvβ8-mediated tumor growth promotion. T_{regs} inhibit expansion of effector $CD8^+$ T cells (57). Our current

and previous studies showed that C6D4 decreased the numbers of T_{regs} and increased the numbers of effector $CD8^+$ T cells in β8-LLC tumors (21).

RNAseq data supported that tumor cells were the major αvβ8-expressing cell type, whereas T cells were the major TGF-β1–expressing cell in the human TME. Cell surface expression of L–TGF-β in non-T_{reg} $CD4^+$ T cells from murine tumors suggests that they are poised to differentiate to pT_{regs} through activation of cell surface L–TGF-β (21). Our data supported a mechanism of T_{reg} enrichment where αvβ8 expression by tumor cells caused L–TGF-β–presenting non-T_{reg} $CD4^+$ T cells to undergo local conversion to pT_{reg}, rather than promoting recruitment of tT_{reg} (Fig. 7, A and B). This conclusion was supported by in vitro studies demonstrating that immobilized or tumor cell αvβ8 drove the conversion of activated T cells to immunosuppressive T_{reg} with low levels of tT_{reg} markers, *Helios* and *Nrp1*, similar to in vivo studies, demonstrating that tumor cell αvβ8 led to the enrichment of pT_{regs}.

Our inability to detect a functional role for αvβ8 expressed by T_{regs} contrasts with other reports proposing a cell-autonomous role for αvβ8 in T_{reg} function using T_{regs} from nontumor sources (44, 45, 58). In these reports, surface expression of αvβ8 is not assessed; rather, the β8 subunit (*itgb8*) was detected by quantitative polymerase chain reaction (qPCR) in murine tT_{reg} and effector T_{reg} populations, which is at very low levels relative to housekeeping genes (44, 45). Such low mRNA expression is consistent with our inability to detect cell-surface αvβ8 because surface expression of αvβ8 is regulated at the level of *itgb8* transcription (59). Thus, although it is possible that, in other tumor systems, αvβ8 can be expressed at functionally significant levels in T_{regs}, our current and past studies, which include surface expression surveys of both tumor and splenic T_{reg}, transcriptomic analysis, and in vitro and in vivo functional assays failed to produce evidence that expression of αvβ8 by T themselves played a role in non-T_{reg} $CD4^+$ T_{reg} cell–to–T_{reg} conversion.

We propose a model (Fig. 7C) to explain why T cells require presentation of L–TGF-β on their cell surface for T_{reg} conversion. In this model, the αvβ8 receptor and its ligand, L–TGF-β/GARP, are concentrated on opposing cell surfaces, not on the same cell surface, and are specifically directed only to the L–TGF-β/GARP–presenting T cell after binding TGF-β signaling (29). This process is more efficient and context-specific than a TGF-βR–bearing T cell encountering active TGF-β diffusing through the extracellular space. Furthermore, this model predicts that if tumor cell αvβ8 binds to either secreted or matrix-bound L–TGF-β, then a TGF-βR–expressing T cell would have to find and orient its receptors to mature TGF-β exposed within the latent complex (Fig. 7C) (29).

Current dogma suggests that actin cytoskeletal force generation through the β-integrin cytoplasmic domain is required to induce conformational changes through the integrin for force generation to L–TGF-β to release TGF-β (42). However, our structural studies show that αvβ8 does not undergo major conformational rearrangements, always remaining in a single extended-closed conformation poised for ligand binding but not force transduction (43, 60). Hence, αvβ8 on cell surfaces is always available for binding to an L–TGF-β–presenting cell, and this binding creates an anchor point to focus the inherent flexibility of L–TGF-β to allow active TGF-β to be sufficiently exposed to bind to its receptors but only on the cell-presenting surface L–TGF-β/GARP (29). Here, we tested this model in vitro

using isolated T cells and showed that T cell TGF-β activation did not require cytoskeletal force transduction from the αvβ8 integrin because the αvβ8 ectodomain immobilized on a solid substrate was freely capable of inducing conversion of contacting non-T_{reg} $CD4^+$ T cells to T_{regs}. This conversion occurred without release and diffusion of TGF-β. The identification of a TGF-β activation mechanism that is diffusion-independent has biologic implications because any L–TGF-β–presenting cell type could potentially increase its TGF-β signaling when contacting an αvβ8-expressing cell (21, 60). Our model also has therapeutic implications because protein-based therapies directed at TGF-β currently in clinical trials are conceptually designed to inhibit diffusible TGF-β (61). Our data indicated that such therapies would poorly target αvβ8-mediated TGF-β activation, while still exposing patients to considerable risk.

Overall, this study highlights a mechanism of T_{reg} enrichment regulated by TGF-β activation in specific tumors that express sufficient levels of αvβ8. We propose that targeting αvβ8 to prevent TGF-β activation will provide a highly effective and more selective approach to overcome T_{reg}-mediated tumor immune evasion in patients with $αvβ8^+$ tumors.

MATERIALS AND METHODS

Study design

This study tested the hypothesis that T_{regs} were required for integrin αvβ8–mediated tumor growth promotion using cell-based assays, in vivo tumor models, and correlative human studies. In vivo models used randomization and blinding maintained until end points were reached and data analysis was completed. Sample sizes for in vitro and in vivo experiments were estimated using power calculations with predetermined effect sizes and variances based on experience.

Mice and orthotopic tumor models

Syngeneic bilateral tumor models were performed in C57BL/6 mice expressing *foxp3*-IRES-GFP [B6.Cg-*FOXP3*tm2(EGFP)Tch/J, Jax] (41) and WT C57BL/6 mice (all female except for TRAMP-C2 experiments using male), 8 to 10 weeks of age, were purchased (the Jackson laboratory), as described (21). See Supplementary Materials and Methods for more information.

Human subjects

Patients were consented for tissue collection under University of California San Francisco Institutional Review Board (UCSF IRB)–approved protocols (UCSF CHR 10–04727, 14–15342, 11–06107, and 10–03413). The study enrollment period started from January 2015 to present, and the sample size was determined by the availability of specimens throughout this period. Samples were selected without regard to prior treatment. Two separate cohorts were developed: the first for cell sorting and RNAseq including samples from gynecologic (n = 53), lung (n = 41), and head and neck squamous cell carcinoma (n = 38) and the second for immunohistochemistry from patients undergoing resection for NSCLC (n = 32).

Study approval

Human tissues were obtained with full approval of the UCSF IRB in full accordance with Declaration of Helsinki principles. Written informed consent was received from participants before inclusion in the study. All animal studies have been approved by the UCSF Institutional Animal Care and Use Committee.

Cell lines

LL/2 (LLC1) [American Type Culture Collection (ATCC), CRL-1642] and TRAMP-C2 (gift from L. Fong, UCSF, San Francisco, CA, USA) were used in TGF-β reporter assays and syngeneic tumor models. OVCAR-3 (UCSF Cell and Genome Engineering Core) and transformed mink lung TGF-β reporter cells (TMLC) (62) were a gift from J. Munger (New York University Medical Center, New York, NY, USA) and were stably transfected with L–TGF-β WT or L–TGF-β (R249A), with or without GARP, as previously described (29). LLC cells were stably transfected to overexpress vector only (mock-LLC) or β8 (β8-LLC) as previously described (21). CHOlec3.2.8.1 (gift from P. Stanley, Albert Einstein College of Medicine, New York, NY, USA), CHO-K1 (ATCC, CCL-61), and human embryonic kidney (HEK) 293 cells (ATCC, CRL-1573) were used for recombinant integrin expression and immunoglobulin G2a (IgG2a) production. All cell lines were maintained in the appropriate media with selection agents and antibiotics, as previously described (21, 29, 43).

Reagents

Anti-CD25 (clone PC-61.5.3) and rat isotype control (HRPN, BP0088) were obtained from Bio X Cell. Anti-β8 (C6D4) is a highly specific engineered recombinant antibody to the specificity determining loop 2 (SDL2) domain of αvβ8 consisting of humanized V genes and CH1 domains, with murine linker and CH2/3 domains in an IgG2a format and is produced in CHO-K1 cells (21, 29). The αvβ8 and αvβ3 ecto-domains were expressed and purified as previously described (43, 60). For all other reagents, see Supplementary Materials and Methods.

DNA constructs

The following PCR products were produced using the following primers and templates: 5′-GATTGTGGGCCCTCTGGGCTCGTCC-GGATTGCTGGTGTTATATTCTTCTGAG-3′ and 5′-CT-GTGGACGCGTATCGCC-3′, human *TGFBR2* expression vector (Sino Biological, HG10358-ACG) and CTCAGAAGAATATAACACCAGCAATCCGGACGAGCCCAGAGGGCCCACAATC and AACGGATCCTCATTTACCCGGAG, mouse IgG2a expression vector. The products were joined by splice overlap extension PCR and cloned into AbVec 2.0 (Addgene, plasmid no. 80795), as described (60). The resulting plasmid was transiently transfected into HEK-293 cells and protein purified as described (21).

Lentiviral transduction

For *itgb8* knockdown, TRAMP-C2 cells were stably transfected with *itgb8*-specific shRNA or nonmammalian control shRNA via lentiviral transduction [Sigma-Aldrich MISSION

lentiviral transduction particles TRCN0000067303 (*itgb8*) or SHC002V (nonmammalian control)].

Isolation, staining, and RNAseq of mouse tumor and immune cells

Mouse tumor immune cell isolation, RNA isolation, and sequencing were performed as described (21). Briefly, mouse tumors were digested; live tumor cells were negatively selected by magnetic beads, or infiltrating lymphoid cells were enriched by density gradient centrifugation. $FOXP3^+$ cells were then sorted from the enriched lymphoid cells by staining with fluorochrome-labeled antibodies as described (21). Total RNA was isolated using kits as described (21), after which cDNA synthesis and amplification were performed. For specific details including library construction and analysis, see Supplementary Materials and Methods.

Isolation, staining, and RNAseq of human tumor and immune cells

Fresh patient tumor samples were dissociated, and the resulting cell suspension was enumerated and stained with the LIVE/DEAD stain and an extracellular antibody cocktail before cell sorting. RNA isolation, cDNA synthesis, library construction, sequencing, and analysis are described in Supplementary Materials and Methods.

T_{reg} maturation assays

Briefly, $CD4^+$ T cells from *foxp3*-IRES-GFP mice were purified and plated onto tissue culture plates coated with αvβ8tr or control substrate [αvβ3tr or bovine serum albumin (BSA)] under T cell stimulation conditions. $CD4^+$ T cells were incubated for 72 hours before phenotyping via flow cytometric analysis. For Transwell diffusion assays, cells were plated into each chamber of the Transwell culture wells containing a 0.4-μm filter using the same conditions as above with further details provided in Supplementary Materials and Methods.

Lymphocyte suppression assays

Cells were cultured as above to create T_{reg} pools and labeled with carboxyfluorescein diacetate succinimidyl ester fluorescent tracking dye exactly as described (63). Labeled cells were stimulated using anti–CD3/CD28 Dynabeads and plated in round-bottom 96-well culture plates. Labeled $CD4^+$ cells were then cocultured with αvβ8-generated T_{regs} or control cells at ratios ranging between 1:1 and 8:1 (labeled $CD4^+$ T cells:T_{regs}). T_{conv} proliferation was measured using flow cytometry after 4 days. For specific details, see Supplementary Materials and Methods.

TGF-β bioassays

TGF-β bioassays were performed as previously described (29) using the cell-intrinsic TGF-β activation reporter system described in (64). Reporter cells were seeded onto culture wells coated with αvβ8tr or control substrate (αvβ3tr or BSA). Cells were incubated for 18 hours before cell lysis and assessment of luciferase activity. For some experiments mock-LLC, β8-LLC, TRAMP-C2, or OVCAR-3 (3×10^4) cells were used in place of immobilized substrates.

Determination of receptor density

CHO WT or CHO transfected with human αvβ8 were plated onto culture plates over a concentration range of 5×10^3 to 30×10^3 cells per well, and recombinant αvβ8 ectodomain [phosphate-buffered saline (10 to 5000 ng/ml)] were coated onto separate wells on the same plate. After cell attachment, cells and coated receptor wells were fixed with 4% paraformaldehyde. Cell-associated or recombinant αvβ8 was detected with clone F9, followed by anti-mouse horseradish peroxidase and colorimetric detection, and cell surface receptor density was determined on the basis of standard curve of estimated recombinant αvβ8 receptor coating efficiency, as described in Supplementary Materials and Methods.

Immunohistochemical analysis of murine and human tumors

Immunohistochemistry was performed as previously described (21). Briefly, prepared formalin-fixed paraffin-embedded (FFPE) sections were stained with anti-mouse β8 (clone F9), B5 (anti-human β8, which does not work in FFPE immunostaining and thus used as isotype control for F9), anti-CD4, anti-CD8, or anti-FOXP3, followed by appropriate detection reagents. For multiplex immunostaining, the Ventana Discovery platform was used as described in Supplementary Materials and Methods.

Quantification and statistical analysis

All data are reported as means ± SEM unless otherwise specified. Comparisons between two different groups were determined using two-tailed Student's *t* test. One-way analysis of variance (ANOVA) was used for multiple comparisons, and Tukey's, Dunnett's, or Sidak's post hoc tests were used to test for statistical significance. Outliers were included unless stated otherwise. Significance was defined as $P < 0.05$. All statistical analyses, including outlier identification (R_{out}), were performed using the software package Prism 7.0b (GraphPad Software).

Supplementary Material

Refer to Web version on PubMed Central for supplementary material.

Acknowledgments:

We thank L. Fong (UCSF, San Francisco, CA, USA) and A. Craig (Queens University, Kingston, ON, Canada) for TRAMP-C2 cells and anti-human and anti-mouse TGF-βR2, respectively.

Funding:

Support was through the NIH (U54HL119893 and R01HL113032 to S.L.N., R01HL134183 to S.L.N. and Y.C., S10OD020054 to Y.C., and P41CA196276 to J.M.) and UC-CAI UCSF Catlyst2 (AB2664) to S.L.N., R01DK093646 (J.L.B.), UCSF Liver Center-P30DK026743 (J.L.B., J.P., S.L.N., and J.M.J.), the Ibrahim El-Hefni Technical Training Foundation (J.L.B.), NIH 1K01DK099405 (J.P.), NIH T32 AI 007334-27 and NIH F31 DK112607 (J.M.J.), and the Howard Hughes Medical Institute (Y.C.).

Competing interests:

S.L.N. and J.M. serve on the Scientific Advisory Board of Venn Therapeutics. S.L.N. is a consultant for Fleet Therapeutics. J.L. is a recipient of sponsored research funds from Venn Therapeutics. The antibodies C6D4 and F9 are included in U.S. Patent application no. 16/331,902 (S.L.N., Y.C., J.M., J.L., J.L.B., and N.T.).

Data and materials availability:

Antibodies and cell lines used in this manuscript will be available upon execution of a material transfer agreement. All other data needed to evaluate the conclusions in the paper are present in the paper or the Supplementary Materials. RNAseq datasets are deposited in the Gene Expression Omnibus (GSE158031).

REFERENCES AND NOTES

1. Fridman WH, Pagès F, Sautès-Fridman C, Galon J, The immune contexture in human tumours: Impact on clinical outcome. Nat. Rev. Cancer12, 298–306 (2012). [PubMed: 22419253]
2. Curiel TJ, Coukos G, Zou L, Alvarez X, Cheng P, Mottram P, Evdemon-Hogan M, Conejo-Garcia JR, Zhang L, Burow M, Zhu Y, Wei S, Kryczek I, Daniel B, Gordon A, Myers L, Lackner A, Disis ML, Knutson KL, Chen L, Zou W, Specific recruitment of regulatory T cells in ovarian carcinoma fosters immune privilege and predicts reduced survival. Nat. Med10, 942–949 (2004). [PubMed: 15322536]
3. Curiel TJ, Tregs and rethinking cancer immunotherapy. J. Clin. Invest117, 1167–1174 (2007). [PubMed: 17476346]
4. Shimizu J, Yamazaki S, Sakaguchi S, Induction of tumor immunity by removing $CD25^{+}CD4^{+}$ T cells: A common basis between tumor immunity and autoimmunity. J. Immunol163, 5211–5218 (1999). [PubMed: 10553041]
5. Onizuka S, Tawara I, Shimizu J, Sakaguchi S, Fujita T, Nakayama E, Tumor rejection by in vivo administration of anti-CD25 (interleukin-2 receptor α) monoclonal antibody. Cancer Res. 59, 3128–3133 (1999). [PubMed: 10397255]
6. Tanaka A, Sakaguchi S, Targeting Treg cells in cancer immunotherapy. Eur. J. Immunol49, 1140–1146 (2019). [PubMed: 31257581]
7. Chen DS, Mellman I, Oncology meets immunology: The cancer-immunity cycle. Immunity39, 1–10 (2013). [PubMed: 23890059]
8. Yadav M, Stephan S, Bluestone JA, Peripherally induced Tregs—Role in immune homeostasis and autoimmunity. Front. Immunol4, 232 (2013). [PubMed: 23966994]
9. Valzasina B, Piconese S, Guiducci C, Colombo MP, Tumor-induced expansion of regulatory T cells by conversion of $CD4^{+}CD25$- lymphocytes is thymus and proliferation independent. Cancer Res. 66, 4488–4495 (2006). [PubMed: 16618776]
10. Paluskievicz CM, Cao X, Abdi R, Zheng P, Liu Y, Bromberg JS, T regulatory cells and priming the suppressive tumor microenvironment. Front. Immunol10, 2453 (2019). [PubMed: 31681327]
11. Ghiringhelli F, Puig PE, Roux S, Parcellier A, Schmitt E, Solary E, Kroemer G, Martin F, Chauffert B, Zitvogel L, Tumor cells convert immature myeloid dendritic cells into TGF-β–secreting cells inducing $CD4^{+}CD25^{+}$ regulatory T cell proliferation. J. Exp. Med202, 919–929 (2005). [PubMed: 16186184]
12. Klein L, Robey EA, Hsieh CS, Central $CD4^{+}$ T cell tolerance: Deletion versus regulatory T cell differentiation. Nat. Rev. Immunol19, 7–18 (2019). [PubMed: 30420705]
13. Anderton MJ, Mellor HR, Bell A, Sadler C, Pass M, Powell S, Steele SJ, Roberts RRA, Heier A, Induction of heart valve lesions by small-molecule ALK5 inhibitors. Toxicol. Pathol39, 916–924 (2011). [PubMed: 21859884]
14. Vitsky A, Waire J, Pawliuk R, Bond A, Matthews D, LaCasse E, Hawes ML, Nelson C, Richards S, Piepenhagen PA, Garman RD, Andrews L, Thurberg BL, Lonning S, Ledbetter S, Ruzek MC, Homeostatic role of transforming growth factor-beta in the oral cavity and esophagus of mice and its expression by mast cells in these tissues. Am. J. Pathol174, 2137–2149 (2009). [PubMed: 19406991]
15. Tolcher AW, Berlin JD, Cosaert J, Kauh J, Chan E, Piha-Paul SA, Amaya A, Tang S, Driscoll K, Kimbung R, Kambhampati SRP, Gueorguieva I, Hong DS, A phase 1 study of anti-TGFβ receptor type-II monoclonal antibody LY3022859 in patients with advanced solid tumors. Cancer Chemother. Pharmacol79, 673–680 (2017). [PubMed: 28280971]

16. Elliott RL, Blobe GC, Role of transforming growth factor Beta in human cancer. J. Clin. Oncol23, 2078–2093 (2005). [PubMed: 15774796]
17. Massagué J, TGFβ in cancer. Cell134, 215–230 (2008). [PubMed: 18662538]
18. Nishimura SL, Integrin-mediated transforming growth factor-β activation, a potential therapeutic target in fibrogenic disorders. Am. J. Pathol175, 1362–1370 (2009). [PubMed: 19729474]
19. Edwards JP, Fujii H, Zhou AX, Creemers J, Unutmaz D, Shevach EM, Regulation of the expression of GARP/latent TGF-β1 complexes on mouse T cells and their role in regulatory T cell and Th17 differentiation. J. Immunol190, 5506–5515 (2013). [PubMed: 23645881]
20. Batlle E, Massagué J, Transforming growth factor-β signaling in immunity and cancer. Immunity50, 924–940 (2019). [PubMed: 30995507]
21. Takasaka N, Seed RI, Cormier A, Bondesson AJ, Lou J, Elattma A, Ito S, Yanagisawa H, Hashimoto M, Ma R, Levine MD, Publicover J, Potts R, Jespersen JM, Campbell MG, Conrad F, Marks JD, Cheng Y, Baron JL, Nishimura SL, Integrin αvβ8–expressing tumor cells evade host immunity by regulating TGF-β activation in immune cells. JCI Insight3, (2018).
22. Stockis J, Roychoudhuri R, Halim TYF, Regulation of regulatory T cells in cancer. Immunology157, 219–231 (2019). [PubMed: 31032905]
23. Mu D, Cambier S, Fjellbirkeland L, Baron JL, Munger JS, Kawakatsu H, Sheppard D, Broaddus VC, Nishimura SL, The integrin αvβ8 mediates epithelial homeostasis through MT1-MMP–dependent activation of TGF-β1. J. Cell Biol157, 493–507 (2002). [PubMed: 11970960]
24. Tanaka A, Sakaguchi S, Regulatory T cells in cancer immunotherapy. Cell Res. 27, 109–118 (2017). [PubMed: 27995907]
25. Aluwihare P, Mu Z, Zhao Z, Yu D, Weinreb PH, Horan GS, Violette SM, Munger JS, Mice that lack activity of αvβ6- and αvβ8-integrins reproduce the abnormalities of *Tgfb1*- and *Tgfb3*-null mice. J. Cell Sci122, 227–232 (2009). [PubMed: 19118215]
26. Yang Z, Mu Z, Dabovic B, Jurukovski V, Yu D, Sung J, Xiong X, Munger JS, Absence of integrin-mediated TGFβ1 activation in vivo recapitulates the phenotype of TGFβ1-null mice. J. Cell Biol176, 787–793 (2007). [PubMed: 17353357]
27. Ozawa A, Sato Y, Imabayashi T, Uemura T, Takagi J, Sekiguchi K, Molecular basis of the ligand binding specificity of αvβ8 integrin. J. Biol. Chem291, 11551–11565 (2016). [PubMed: 27033701]
28. Kitamura H, Cambier S, Somanath S, Barker T, Minagawa S, Markovics J, Goodsell A, Publicover J, Reichardt L, Jablons D, Wolters P, Hill A, Marks JD, Lou J, Pittet JF, Gauldie J, Baron JL, Nishimura SL, Mouse and human lung fibroblasts regulate dendritic cell trafficking, airway inflammation, and fibrosis through integrin αvβ8–mediated activation of TGF-β. J. Clin. Invest121, 2863–2875 (2011). [PubMed: 21646718]
29. Campbell MG, Cormier A, Ito S, Seed RI, Bondesson AJ, Lou J, Marks JD, Baron JL, Cheng Y, Nishimura SL, Cryo-EM reveals integrin-mediated TGF-β activation without release from latent TGF-β. Cell180, 490–501.e16 (2020). [PubMed: 31955848]
30. Arce Vargas F, Furness AJS, Solomon I, Joshi K, Mekkaoui L, Lesko MH, Miranda Rota E, Dahan R, Georgiou A, Sledzinska A, Ben Aissa A, Franz D, Werner Sunderland M, Wong YNS, Henry JY, O'Brien T, Nicol D, Challacombe B, Beers SA, Turajlic S, Gore M, Larkin J, Swanton C, Chester KA, Pule M, Ravetch JV, Marafioti T, Peggs KS, Quezada SA, Spain L, Wotherspoon A, Francis N, Smith M, Strauss D, Hayes A, Soultati A, Stares M, Spain L, Lynch J, Fotiadis N, Fernando A, Hazell S, Chandra A, Pickering L, Rudman S, Chowdhury S, Swanton C, Jamal-Hanjani M, Veeriah S, Shafi S, Czyzewska-Khan J, Johnson D, Laycock J, Bosshard-Carter L, Goh G, Rosenthal R, Gorman P, Murugaesu N, Hynds RE, Wilson G, Birkbak NJ, Watkins TBK, McGranahan N, Horswell S, Mitter R, Escudero M, Stewart A, van Loo P, Rowan A, Xu H, Turajlic S, Hiley C, Abbosh C, Goldman J, Stone RK, Denner T, Matthews N, Elgar G, Ward S, Biggs J, Costa M, Begum S, Phillimore B, Chambers T, Nye E, Graca S, al Bakir M, Hartley JA, Lowe HL, Herrero J, Lawrence D, Hayward M, Panagiotopoulos N, Kolvekar S, Falzon M, Borg E, Simeon C, Hector G, Smith A, Aranda M, Novelli M, Oukrif D, Janes SM, Thakrar R, Forster M, Ahmad T, Lee SM, Papadatos-Pastos D, Carnell D, Mendes R, George J, Navani N, Ahmed A, Taylor M, Choudhary J, Summers Y, Califano R, Taylor P, Shah R, Krysiak P, Rammohan K, Fontaine E, Booton R, Evison M, Crosbie P, Moss S, Idries F, Joseph L, Bishop P, Chaturved A, Quinn AM, Doran H, Leek A, Harrison P, Moore K, Waddington R, Novasio J,

Blackhall F, Rogan J, Smith E, Dive C, Tugwood J, Brady G, Rothwell DG, Chemi F, Pierce J, Gulati S, Naidu B, Langman G, Trotter S, Bellamy M, Bancroft H, Kerr A, Kadiri S, Webb J, Middleton G, Djearaman M, Fennell D, Shaw JA, le Quesne J, Moore D, Nakas A, Rathinam S, Monteiro W, Marshall H, Nelson L, Bennett J, Riley J, Primrose L, Martinson L, Anand G, Khan S, Amadi A, Nicolson M, Kerr K, Palmer S, Remmen H, Miller J, Buchan K, Chetty M, Gomersall L, Lester J, Edwards A, Morgan F, Adams H, Davies H, Kornaszewska M, Attanoos R, Lock S, Verjee A, MacKenzie M, Wilcox M, Bell H, Iles N, Hackshaw A, Ngai Y, Smith S, Gower N, Ottensmeier C, Chee S, Johnson B, Alzetani A, Shaw E, Lim E, de Sousa P, Barbosa MT, Bowman A, Jorda S, Rice A, Raubenheimer H, Proli C, Cufari ME, Ronquillo JC, Kwayie A, Bhayani H, Hamilton M, Bakar Y, Mensah N, Ambrose L, Devaraj A, Buderi S, Finch J, Azcarate L, Chavan H, Green S, Mashinga H, Nicholson AG, Lau K, Sheaff M, Schmid P, Conibear J, Ezhil V, Ismail B, Irvin-sellers M, Prakash V, Russell P, Light T, Horey T, Danson S, Bury J, Edwards J, Hill J, Matthews S, Kitsanta Y, Suvarna K, Fisher P, Keerio AD, Shackcloth M, Gosney J, Postmus P, Feeney S, Asante-Siaw J, Fc-optimized anti-CD25 depletes tumor-infiltrating regulatory T cells and synergizes with PD-1 blockade to eradicate established tumors. Immunity46, 577–586 (2017). [PubMed: 28410988]

31. Pincetic A, Bournazos S, DiLillo DJ, Maamary J, Wang TT, Dahan R, Fiebiger BM, Ravetch JV, Type I and type II Fc receptors regulate innate and adaptive immunity. Nat. Immunol15, 707–716 (2014). [PubMed: 25045879]
32. Thornton AM, Lu J, Korty PE, Kim YC, Martens C, Sun PD, Shevach EM, Helios^{+} and Helios^{-} Treg subpopulations are phenotypically and functionally distinct and express dissimilar TCR repertoires. Eur. J. Immunol49, 398–412 (2019). [PubMed: 30620397]
33. Landuyt AE, Klocke BJ, Colvin TB, Schoeb TR, Maynard CL, Cutting edge: ICOS-deficient regulatory T cells display normal induction of *Il10* but readily downregulate expression of Foxp3. J. Immunol202, 1039–1044 (2019). [PubMed: 30642977]
34. Ondondo B, Jones E, Godkin A, Gallimore A, Home sweet home: The tumor microenvironment as a haven for regulatory T cells. Front. Immunol4, 197 (2013). [PubMed: 23874342]
35. Bruder D, Probst-Kepper M, Westendorf AM, Geffers R, Beissert S, Loser K, von Boehmer H, Buer J, Hansen W, Neuropilin-1: A surface marker of regulatory T cells. Eur. J. Immunol34, 623–630 (2004). [PubMed: 14991591]
36. Thornton AM, Korty PE, Tran DQ, Wohlfert EA, Murray PE, Belkaid Y, Shevach EM, Expression of Helios, an Ikaros transcription factor family member, differentiates thymic-derived from peripherally induced Foxp3^{+} T regulatory cells. J. Immunol184, 3433–3441 (2010). [PubMed: 20181882]
37. Weiss JM, Bilate AM, Gobert M, Ding Y, Curotto de Lafaille MA, Parkhurst CN, Xiong H, Dolpady J, Frey AB, Ruocco MG, Yang Y, Floess S, Huehn J, Oh S, Li MO, Niec RE, Rudensky AY, Dustin ML, Littman DR, Lafaille JJ, Neuropilin 1 is expressed on thymus-derived natural regulatory T cells, but not mucosa-generated induced Foxp3^{+} T reg cells. J. Exp. Med209, 1723–1742 (2012). [PubMed: 22966001]
38. Yadav M, Louvet C, Davini D, Gardner JM, Martinez-Llordella M, Bailey-Bucktrout S, Anthony BA, Sverdrup FM, Head R, Kuster DJ, Ruminski P, Weiss D, Schack DV, Bluestone JA, Neuropilin-1 distinguishes natural and inducible regulatory T cells among regulatory T cell subsets in vivo. J. Exp. Med209, 1713–1722 (2012). [PubMed: 22966003]
39. Oida T, Weiner HL, TGF-β induces surface LAP expression on murine CD4 T cells independent of Foxp3 induction. PLOS ONE5, e15523 (2010). [PubMed: 21124798]
40. Nakamura K, Kitani A, Strober W, Cell contact–dependent immunosuppression by CD4^{+}CD25^{+} regulatory T cells is mediated by cell surface–bound transforming growth factor β. J. Exp. Med194, 629–644 (2001). [PubMed: 11535631]
41. Haribhai D, Lin W, Relland LM, Truong N, Williams CB, Chatila TA, Regulatory T cells dynamically control the primary immune response to foreign antigen. J. Immunol178, 2961–2972 (2007). [PubMed: 17312141]
42. Dong X, Zhao B, Iacob RE, Zhu J, Koksal AC, Lu C, Engen JR, Springer TA, Force interacts with macromolecular structure in activation of TGF-β. Nature542, 55–59 (2017). [PubMed: 28117447]

43. Cormier A, Campbell MG, Ito S, Wu S, Lou J, Marks J, Baron JL, Nishimura SL, Cheng Y, Cryo-EM structure of the αvβ8 integrin reveals a mechanism for stabilizing integrin extension. Nat. Struct. Mol. Biol25, 698–704 (2018). [PubMed: 30061598]
44. Edwards JP, Thornton AM, Shevach EM, Release of active TGF-β1 from the latent TGF-β1/GARP complex on T regulatory cells is mediated by integrin β8. J. Immunol193, 2843–2849 (2014). [PubMed: 25127859]
45. Worthington JJ, Kelly A, Smedley C, Bauché D, Campbell S, Marie JC, Travis MA, Integrin αvβ8-mediated TGF-β activation by effector regulatory T cells is essential for suppression of T-cell-mediated inflammation. Immunity42, 903–915 (2015). [PubMed: 25979421]
46. Azhar M, Yin M, Bommireddy R, Duffy JJ, Yang J, Pawlowski SA, Boivin GP, Engle SJ, Sanford LP, Grisham C, Singh RR, Babcock GF, Doetschman T, Generation of mice with a conditional allele for transforming growth factor beta 1 gene. Genesis47, 423–431 (2009). [PubMed: 19415629]
47. Thomas DA, Massagué J, TGF-beta directly targets cytotoxic T cell functions during tumor evasion of immune surveillance. Cancer Cell8, 369–380 (2005). [PubMed: 16286245]
48. Donkor MK, Sarkar A, Li MO, Tgf-β1 produced by activated $CD4^{+}$T cells antagonizes T cell surveillance of tumor development. Onco. Targets. Ther1, 162–171 (2012).
49. Salem M, Wallace C, Velegraki M, Li A, Ansa-Addo E, Metelli A, Kwon H, Riesenberg B, Wu B, Zhang Y, Guglietta S, Sun S, Liu B, Li Z, GARP dampens cancer immunity by sustaining function and accumulation of regulatory T cells in the colon. Cancer Res. 79, 1178–1190 (2019). [PubMed: 30674536]
50. Moulin A, Mathieu M, Lawrence C, Bigelow R, Levine M, Hamel C, Marquette JP, le Parc J, Loux C, Ferrari P, Capdevila C, Dumas J, Dumas B, Rak A, Bird J, Qiu H, Pan CQ, Edmunds T, Wei RR, Structures of a pan-specific antagonist antibody complexed to different isoforms of TGFβ reveal structural plasticity of antibody-antigen interactions. Protein Sci. 23, 1698–1707 (2014). [PubMed: 25209176]
51. Lienart S, Merceron R, Vanderaa C, Lambert F, Colau D, Stockis J, van der Woning B, De Haard H, Saunders M, Coulie PG, Savvides SN, Lucas S, Structural basis of latent TGF-β1 presentation and activation by GARP on human regulatory T cells. Science362, 952–956 (2018). [PubMed: 30361387]
52. Gabriely G, da Cunha AP, Rezende RM, Kenyon B, Madi A, Vandeventer T, Skillin N, Rubino S, Garo L, Mazzola MA, Kolypetri P, Lanser AJ, Moreira T, Faria AMC, Lassmann H, Kuchroo V, Murugaiyan G, Weiner HL, Targeting latency-associated peptide promotes antitumor immunity. Sci. Immunol2, eaaj1738 (2017). [PubMed: 28763794]
53. Gavin MA, Torgerson TR, Houston E, deRoos P, Ho WY, Stray-Pedersen A, Ocheltree EL, Greenberg PD, Ochs HD, Rudensky AY, Single-cell analysis of normal and FOXP3-mutant human T cells: FOXP3 expression without regulatory T cell development. Proc. Natl. Acad. Sci. U.S.A103, 6659–6664 (2006). [PubMed: 16617117]
54. Pratama A, Schnell A, Mathis D, Benoist C, Developmental and cellular age direct conversion of CD4+ T cells into $ROR\gamma^{+}$ or $Helios^{+}$ colon Treg cells. J. Exp. Med217, e20190428 (2020). [PubMed: 31685531]
55. Ahmadzadeh M, Pasetto A, Jia L, Deniger DC, Stevanović S, Robbins PF, Rosenberg SA, Tumor-infiltrating human $CD4^{+}$ regulatory T cells display a distinct TCR repertoire and exhibit tumor and neoantigen reactivity. Sci. Immunol4, eaao4310 (2019). [PubMed: 30635355]
56. Plitas G, Konopacki C, Wu K, Bos PD, Morrow M, Putintseva EV, Chudakov DM, Rudensky AY, Regulatory T cells exhibit distinct features in human breast cancer. Immunity45, 1122–1134 (2016). [PubMed: 27851913]
57. Kastenmuller W, Gasteiger G, Subramanian N, Sparwasser T, Busch DH, Belkaid Y, Drexler I, Germain RN, Regulatory T cells selectively control $CD8^{+}$ T cell effector pool size via IL-2 restriction. J. Immunol187, 3186–3197 (2011). [PubMed: 21849683]
58. Stockis J, Liénart S, Colau D, Collignon A, Nishimura SL, Sheppard D, Coulie PG, Lucas S, Blocking immunosuppression by human Tregs in vivo with antibodies targeting integrin αVβ8. Proc. Natl. Acad. Sci. U.S.A114, E10161–E10168 (2017). [PubMed: 29109269]

59. Markovics JA, Araya J, Cambier S, Jablons D, Hill A, Wolters PJ, Nishimura SL, Transcription of the transforming growth factor beta activating integrin beta8 subunit is regulated by SP3, AP-1, and the p38 pathway. J. Biol. Chem285, 24695–24706 (2010). [PubMed: 20519498]
60. Minagawa S, Lou J, Seed RI, Cormier A, Wu S, Cheng Y, Murray L, Tsui P, Connor J, Herbst R, Govaerts C, Barker T, Cambier S, Yanagisawa H, Goodsell A, Hashimoto M, Brand OJ, Cheng R, Ma R, Knelly KJM, Wen W, Hill A, Jablons D, Wolters P, Kitamura H, Araya J, Barczak AJ, Erle DJ, Reichardt LF, Marks JD, Baron JL, Nishimura SL, Selective targeting of TGF-β activation to treat fibroinflammatory airway disease. Sci. Transl. Med6, 241ra79 (2014).
61. Derynck R, Turley SJ, Akhurst RJ, TGFβ biology in cancer progression and immunotherapy. Nat. Rev. Clin. Oncol18, 9–34 (2021). [PubMed: 32710082]
62. Abe M, Harpel JG, Metz CN, Nunes I, Loskutoff DJ, Rifkin DB, An assay for transforming growth factor-beta using cells transfected with a plasminogen activator inhibitor-1 promoter-luciferase construct. Anal. Biochem216, 276–284 (1994). [PubMed: 8179182]
63. Lim JF, Berger H, Su IH, Isolation and activation of murine lymphocytes. J. Vis. Exp, 54596 (2016).
64. Shi M, Zhu J, Wang R, Chen X, Mi L, Walz T, Springer TA, Latent TGF-β structure and activation. Nature474, 343–349 (2011). [PubMed: 21677751]
65. Khan SA, Joyce J, Tsuda T, Quantification of active and total transforming growth factor-β levels in serum and solid organ tissues by bioassay. BMC. Res. Notes5, 636 (2012). [PubMed: 23151377]
66. Radaev S, Zou Z, Huang T, Lafer EM, Hinck AP, Sun PD, Ternary complex of transforming growth factor-beta1 reveals isoform-specific ligand recognition and receptor recruitment in the superfamily. J. Biol. Chem285, 14806–14814 (2010). [PubMed: 20207738]
67. Newsted D, Banerjee S, Watt K, Nersesian S, Truesdell P, Blazer LL, Cardarelli L, Adams JJ, Sidhu SS, Craig AW, Blockade of TGF-β signaling with novel synthetic antibodies limits immune exclusion and improves chemotherapy response in metastatic ovarian cancer models. Onco. Targets. Ther8, e1539613 (2018).
68. Hartigan-O'Connor DJ, Poon C, Sinclair E, McCune JM, Human CD4+ regulatory T cells express lower levels of the IL-7 receptor alpha chain (CD127), allowing consistent identification and sorting of live cells. J. Immunol. Methods319, 41–52 (2007). [PubMed: 17173927]
69. Conesa A, Madrigal P, Tarazona S, Gomez-Cabrero D, Cervera A, McPherson A, Szcześniak MW, Gaffney DJ, Elo LL, Zhang X, Mortazavi A, A survey of best practices for RNA-seq data analysis. Genome Biol. 17, 13 (2016). [PubMed: 26813401]
70. Dobin A, Davis CA, Schlesinger F, Drenkow J, Zaleski C, Jha S, Batut P, Chaisson M, Gingeras TR, STAR: Ultrafast universal RNA-seq aligner. Bioinformatics29, 15–21 (2013). [PubMed: 23104886]
71. Li B, Dewey CN, RSEM: Accurate transcript quantification from RNA-Seq data with or without a reference genome. BMC Bioinformatics12, 323 (2011). [PubMed: 21816040]
72. Sorensen K, Brodbeck U, Assessment of coating-efficiency in ELISA plates by direct protein determination. J. Immunol. Methods95, 291–293 (1986). [PubMed: 3794350]
73. Zemmour D, Zilionis R, Kiner E, Klein AM, Mathis D, Benoist C, Single-cell gene expression reveals a landscape of regulatory T cell phenotypes shaped by the TCR. Nat. Immunol19, 291–301 (2018). [PubMed: 29434354]

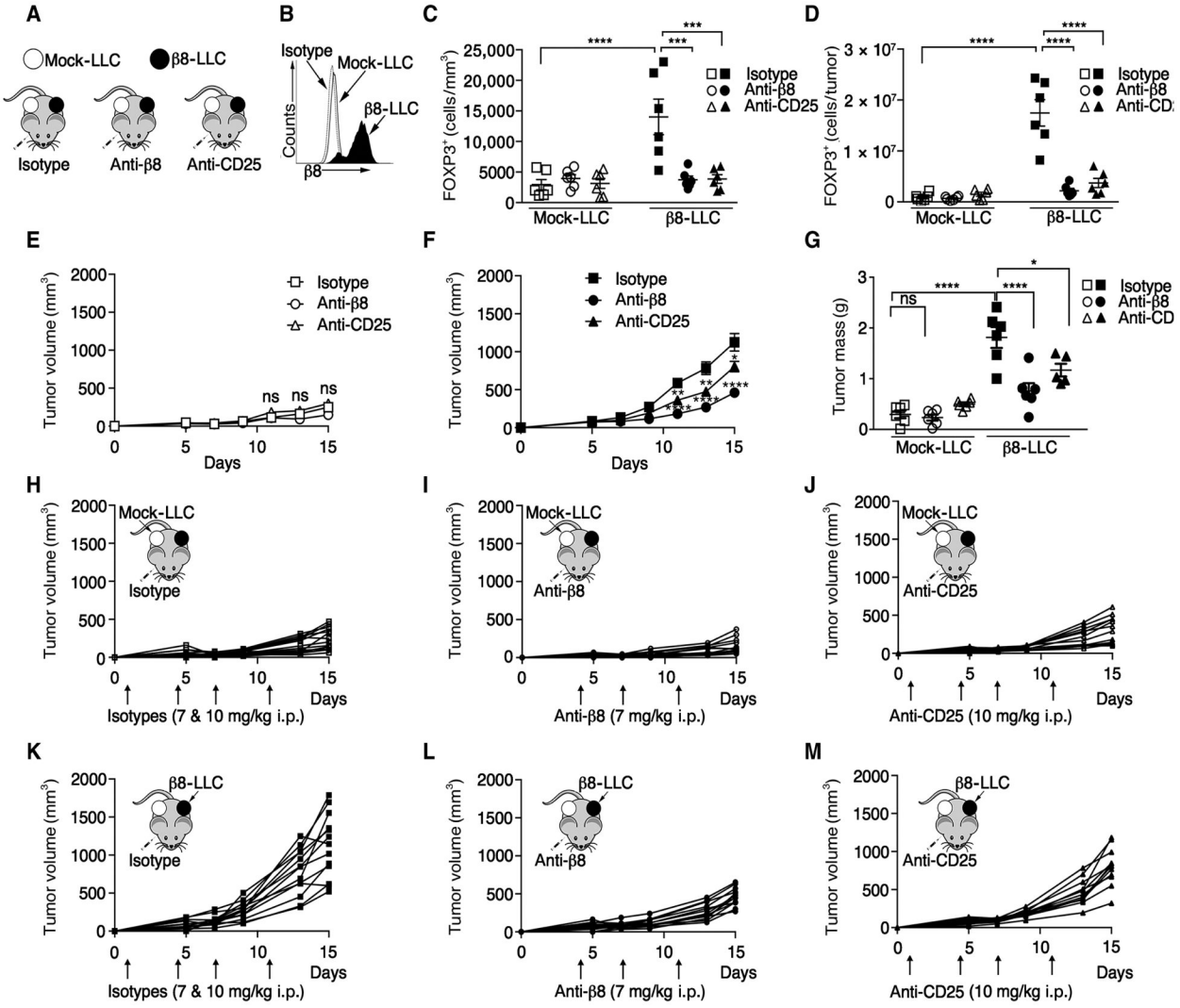

Fig. 1. T_{reg} depletion specifically inhibited β8-LLC but not mock-LLC tumor outgrowth.

(**A**) Cartoon of tumor model. (**B**) Representative surface staining: anti-β8 (C6D4) or isotype control of mock-LLC or β8-LLC cells. (**C** to **M**) Mock-LLC and β8-LLC tumors were established on opposing flanks of C57BL/6 mice. (C to G, I, and L) Mice were treated [7 mg/kg, intraperitoneally (i.p.)] with anti-β8 (C6D4) after tumor establishment. (J and M) T_{regs} were depleted with anti-CD25 (clone PC-61.5.3) starting 1 day after tumor cell injection. (H and K) Isotype controls. (C and D) Intratumoral T_{reg} numbers (outliers removed) confirmed by immunohistochemistry of FOXP3 of mock (open) or β8-LLC (filled) tumors shown by $FOXP3^+$ cells/tumor surface area I or $FOXP3^+$ cells/tumor (D). Average LLC tumor volumes for mock-LLC (E) and β8-LLC (F), with day 15 tumor weights (G). Corresponding spider plots for mock-LLC (H to J) treated with isotype (H), anti-β8, C6D4 (I), anti-CD25 (J), or β8-LLC treated with isotype (K), anti-β8, C6D4 (L), or anti-CD25 (M). Arrows indicate antibody injection days. (H to M) Cartoons show tumor type (arrow) in accompanying plots. One-way ANOVA was used for multiple comparisons followed by Tukey's post-test. Student's unpaired *t* test was used for comparing two

datasets. Shown is SE, *$P < 0.05$, **$P < 0.01$, ***$P < 0.001$, and ****$P < 0.0001$. ns, not significant.

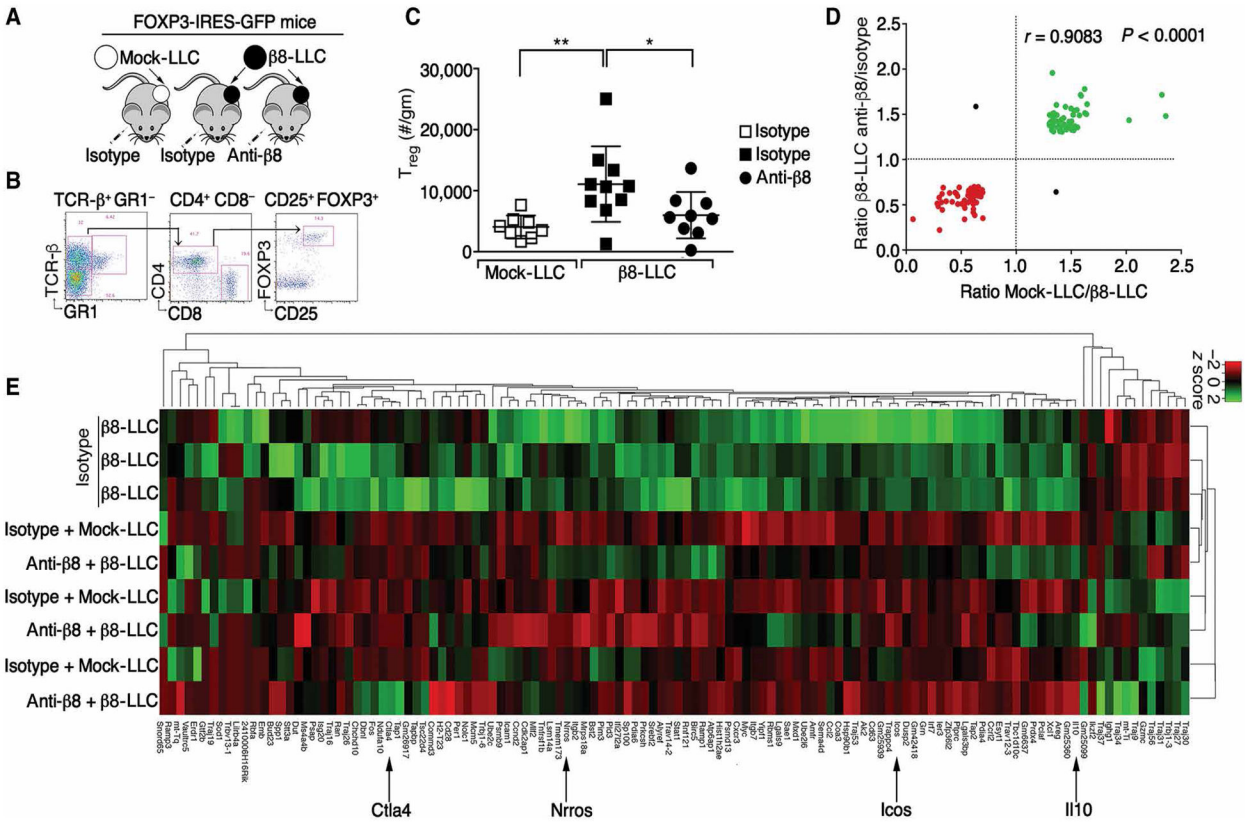

Fig. 2. Tumor cell expression of αvβ8 drove a distinct immunosuppressive T_{reg}transcriptome. (**A**) Cartoon of model. (**B**) Gating strategy for $FOXP3^+CD25^+$ cells, enumerated in (**C**) as $FOXP3^+CD25^+$ cells/g (outliers removed) of mock (open boxes) or β8-LLC tumors treated with isotype (filled boxes) or anti-β8 (C6D4, filled circles). (**D**) Bulk RNAseq of sorted pools (9 to 10 mice per group in three pools) of $CD4^+GFP^+$ cells. Differential expression plot of 118 most highly expressed genes [>50 average fragments per kilobase million (FKPM)] increased (green) or decreased (red) in expression by at least 30% in T_{reg} groups treated with anti-β8 compared with isotype control or mock-LLC compared with β8-LLC, with Pearson *R* and two tailed *P* value. (**E**) Hierarchal clustering and heatmap of 118 most highly and variably expressed genes shown in (D). Note that T_{regs} from β8-LLC isotype–treated tumors are distinct (top three rows) from mock or β8-LLC T_{reg} treated with anti-β8 (C6D4). Arrows indicate key genes. For multiple comparisons, one-way ANOVA was used followed by Tukey's post-test. $*P < 0.05$ and $**P < 0.01$.

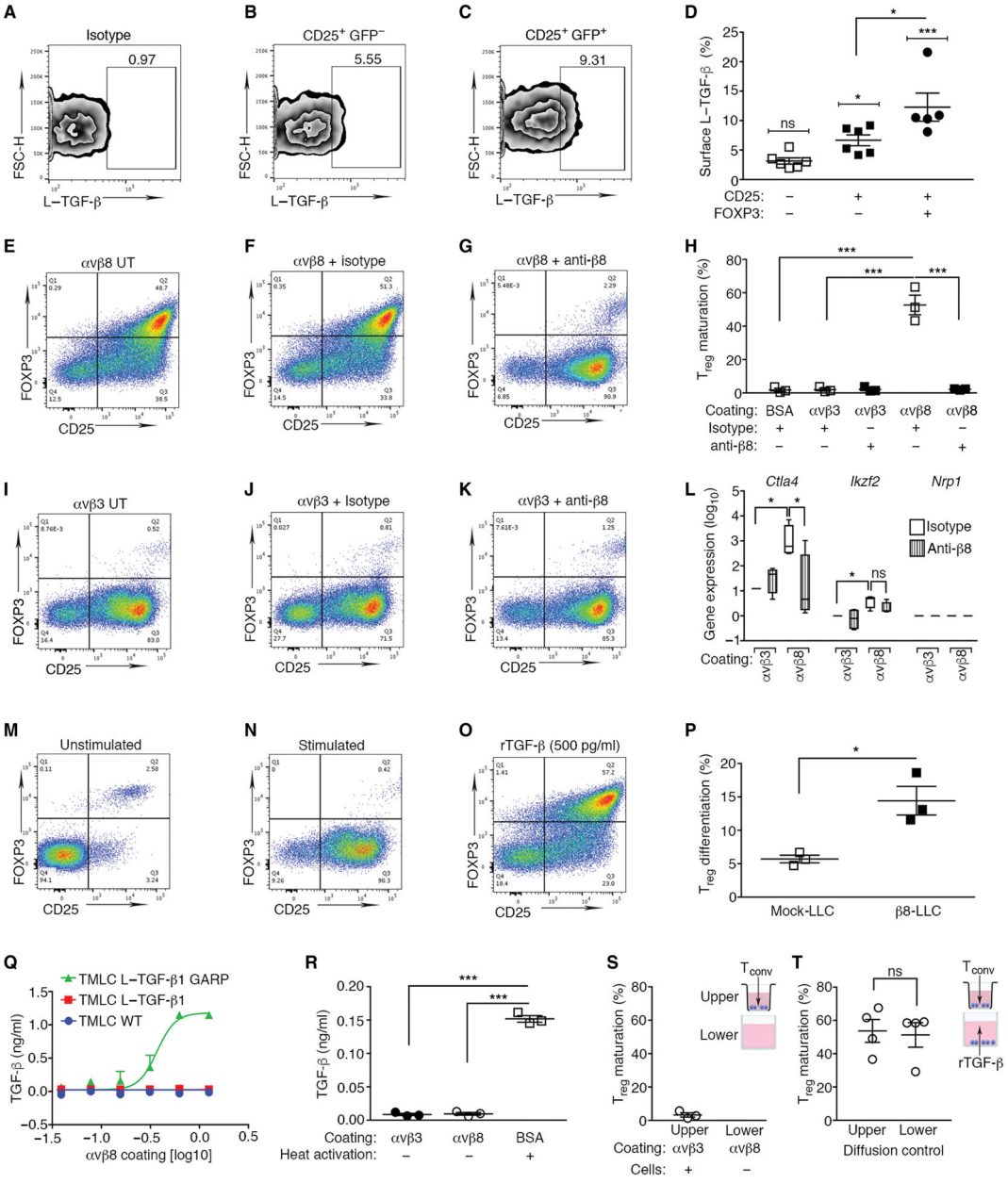

Fig. 3. Contact of L–TGF-β–presenting non-T_{reg} CD4$^+$ T cells with αvβ8 drove iT_{reg} differentiation.

(**A** to **C**) CD4$^+$ mouse splenocytes express L–TGF-β1 on the cell surface. (A) Isotype-matched negative control for (B) CD4$^+$CD25$^+$ FOXP3$^-$ T cells and (C) CD4$^+$CD25$^+$ FOXP3$^+$ T_{reg} stained with anti-LAP. (**D**) L–TGF-β1 surface staining (outlier removed) in CD4$^+$CD25$^-$FOXP3$^-$, CD4$^+$CD25$^+$FOXP3$^-$, and CD4$^+$CD25$^+$ FOXP3$^+$ T cell subsets (brackets above each column indicate comparisons relative to isotype control). (**E** to **G**) CD4$^+$ mouse splenocytes undergo iT_{reg} differentiation when cultured on immobilized αvβ8, but not on (**I** to **K**) integrin αvβ3, or on (**M** and **N**) BSA. (E to K and N) CD4$^+$ splenocytes from *FOXP3*-IRES-GFP mice were activated [anti-CD3 and interleukin (IL-2)] or (M) not stimulated. (**O**) As positive control, stimulated CD4$^+$ T cells were treated

with supraphysiologic levels of rTGF-β1 (500 pg/ml) (65). Representative experiment (n = 3) depicts $CD4^+$ gated T cells stained with anti-CD25 (x axis) with FOXP3 expression determined by green fluorescent protein (GFP; y axis).T_{reg} ($CD4^+CD25^+$ GFP^+, upper right quadrant). Gating strategy is shown in fig. S3 (A to D). (E and I) Individual wells were untreated (UT), treated with isotype (F and J), or anti-β8 and C6D4 (1 μg/ml) (G and K). (H) Lower column (n = 3) coating substrate indicated as BSA, αvβ3, or αvβ8. (L) *Ctla4*, *Ikzf2*, or *Nrp1* expression determined by qPCR demonstrates αvβ8-dependent T_{reg} differentiation under identical culture conditions as in (F, G, J, and K). Results (log_{10}) normalized to αvβ3 controls. Treatment with isotype (open) or C6D4 (vertically striped) are indicated. (**P**) Activated T cells cocultured with mock or β8-LLC cells significantly increased T_{reg} differentiation compared with coculture with mock-LLC controls. (**Q**) TGF-β activation over range of αvβ8 coating concentrations reported by WT TMLC (blue), L–TGF-β1–transfected TMLC (red), or L–TGF-β1/GARP–transfected TMLC cells (green). (**R**) L–TGF-β within conditioned media of T_{conv} cultured under stimulatory conditions for 48 hours identical to conditions in (N). Reporter cells plated on control substrate αvβ3 or αvβ8 with secreted L–TGF-β. Heat (80°C) activation of conditioned media showed total amount of L–TGF-β present. (**S**) Transwell assay determined the importance of cell contact in αvβ8-mediated T_{reg} differentiation. αvβ8 was coated on the lower chambers. $CD4^+$ T cells were plated only into the upper chambers under stimulating conditions (IL-2 and anti-CD3). The upper chamber Transwell surface contains 0.4-μm pores, allowing diffusion of soluble mediators from the lower chamber, but not cells. (**T**) Active rTGF-β added to the medium in the lower chamber demonstrates that TGF-β freely diffuses from the lower to the upper chamber to induce $CD25^+FOXP3^+$ T_{reg} differentiation. $*P < 0.05$ and $***P < 0.001$ by one-way ANOVA for multiple comparisons followed by Sidak's post-test or unpaired Student's t test to compare two populations.

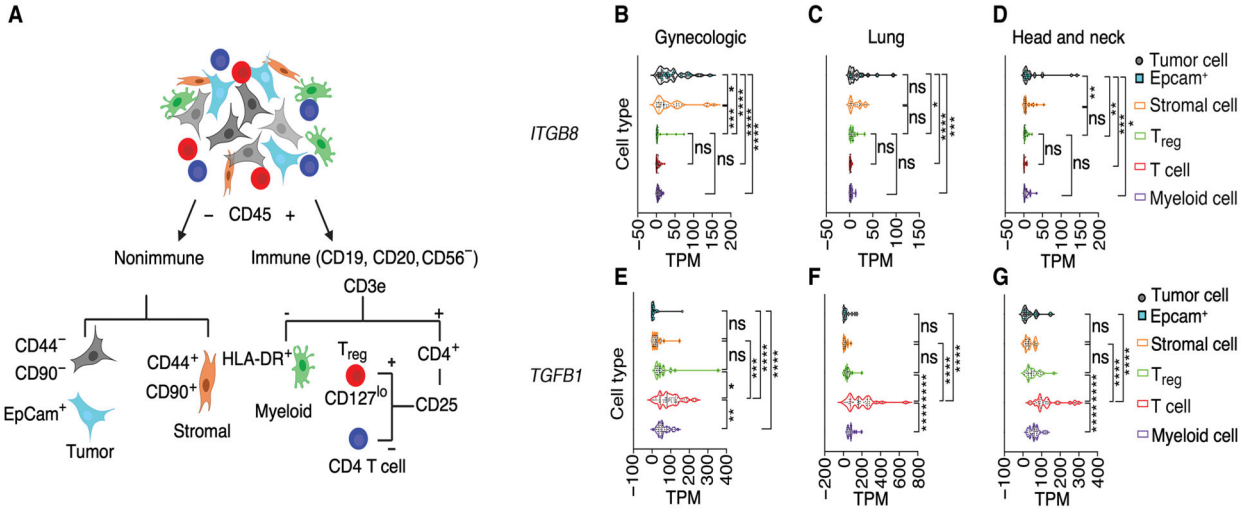

Fig. 4. *ITGB8* was highly expressed in tumor cells, and *TGFB1* was highly expressed in immune cells.

(**A**) Schematic of sorting strategy to purify tumor, stromal, myeloid, $CD4^+$ T cell, and $CD4^+CD25^+CD127^{lo}$ T_{reg} populations from disaggregated human tumors. (**B** to **G**). Bulk RNAseq performed on sorted cell populations from cohorts of human gynecologic (n = 53), non–small cell lung carcinoma (n = 41), or head and neck cancer specimens (n = 38) represented as transcript per million (TPM) (normalized read counts to gene length and scaling 1×10^6). Violin plots of normalized TPM of (B to D) *ITGB8* and (E to G) *TGFB1* of $CD44^-CD90^-$ tumor cells (gray circles), some of which stain with anti-epithelial cell adhesion molecule (EpCam) (blue filled squares), $CD44^+CD90^+$ stromal cells (filled circles), $CD4^+CD25^+$ T_{reg} (green) or $CD4^+$ T cells (red), or major histocompatibility complex class II ($MHCII^+$) (human leukocyte antigen DR isotype, $HLA\text{-}DR^+$) myeloid cells (purple). All data points were included in the analysis without outlier exclusion and were analyzed for significance by one-way ANOVA for multiple comparisons followed by Dunnett's post-test; means ± SD. ns, $P > 0.05$; $^*P < 0.05$, $^{**}P < 0.01$, $^{***}P < 0.001$, and $^{****}P < 0.0001$.

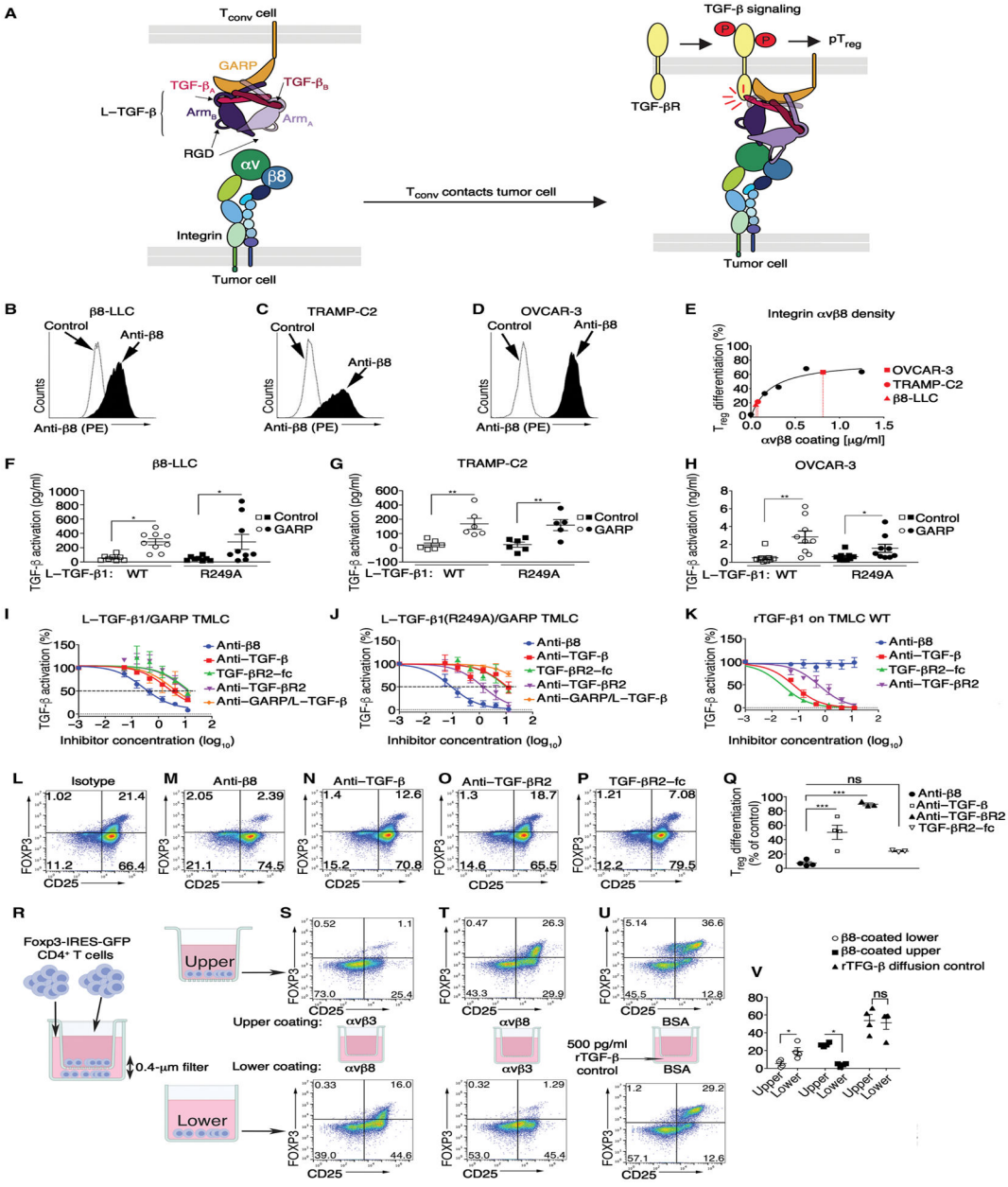

Fig. 5. Formation of a localized tumor/T cell αvβ8/L–TGF-β signaling complex.

(**A**) Cartoon of structure-based model of αvβ8-mediated TGF-β activation and signaling based on structures of αvβ8/L–TGF-β (29, 43), L–TGF-β/GARP (51), and TGF-βR2/TGF-β1 (66). Integrin αv and β8 subunits, latency associated peptide (LAP) of dimeric L–TGF-β (subunit A + B), dimeric TGF-β (subunit A + B), TGF-βR2, and GARP color-coded matching annotations. Integrin and GARP/TGF-βR2 trans-membrane domains span tumor or T_{reg} lipid bilayers, respectively. (**B**) αvβ8 surface expression in β8-LLC, (**C**) TRAMP-C2, and (**D**) OVCAR-3 stained with C6D4 (1 μg/ml) compared with iso-type. (**E**) T_{reg} differentiation over a range of αvβ8 coating concentrations. Superimposed in red are β8-LLC (red triangle), TRAMP-C2 (red circle), and OVCAR-3 (red square) according to calculated αvβ8 cell surface receptor density. (**F** to **H**) WT human L–TGF-β1 or mutant

incapable of producing diffusible TGF-β1 [L–TGF-β1(R249A)] expressed alone (square symbols) or coexpressed with human GARP (circles) in TGF-β reporter cells (TMLC) and cocultured with (F) β8-LLC, (G) TRAMP-C2, or (H) OVCAR-3. Outliers (R_{out}) were removed from (F and G). Shown is TGF-β activation (means ± SEM) determined using rTGF-β standard curve of each TMLC line ($n \geq 6$). (**I** to **K**) Inhibition curves of anti-β8 (C6D4, blue line) compared with anti–pan–TGF-β (1D11, red line), TGF-βR2–Fc receptor trap (green line), anti-human GARP/L–TGF-β (MHG-8, purple line), or anti-human/mouse TGF-βR2 (clone 8322, orange line) generated using (I) WT human L–TGF-β1/human GARP TMLC, (J) human L–TGF-β1(R249A)/human GARP TMLC or control, and (K) WT TMLC cells with 500 pg of rTGF-β1. Shown is percent inhibition relative to no antibody control. Inhibitor concentrations are shown in μg/ml ($\log_{10}$). (**L** to **P**) iT_{reg} differentiation of activated $CD4^+$ T cells from *foxp3*-IRES-GFP splenocytes on immobilized αvβ8 in the presence of (L) isotype, (M) anti-β8 (C6D4), (N) anti–TGF-β1 (1D11), (O) anti–TGF-βR2 (clone 8322), (P) or TGF-βR2–Fc. (**Q**) Results enumerated in scatterplots ($n \geq 3$). (**R**) Schematic of Transwell assay showing that diffusible TGF-β has no role in αvβ8-mediated iT_{reg} differentiation. $CD4^+$ T cells plated into upper and lower chambers under stimulating conditions. (**S**) αvβ8 coated on lower, αvβ3 control on upper, or (**T**) vice versa. (**U**) Active rTGF-β added to lower chamber media demonstrating diffusion of rTGF-β into the upper chamber inducing conversion of non-T_{reg} $CD4^+$ T cells (T_{conv}) to $CD25^+FOXP3^+$ T_{reg}. (**V**) Scatterplots ($n = 4$) show gated $CD4^+$ T cells stained with anti-CD25 (*x* axis) with FOXP3 expression determined by GFP (*y* axis). $^*P < 0.05$, $^{**}P < 0.01$, and $^{***}P < 0.001$ by one-way ANOVA for multiple comparisons followed by Sidak's post-test.

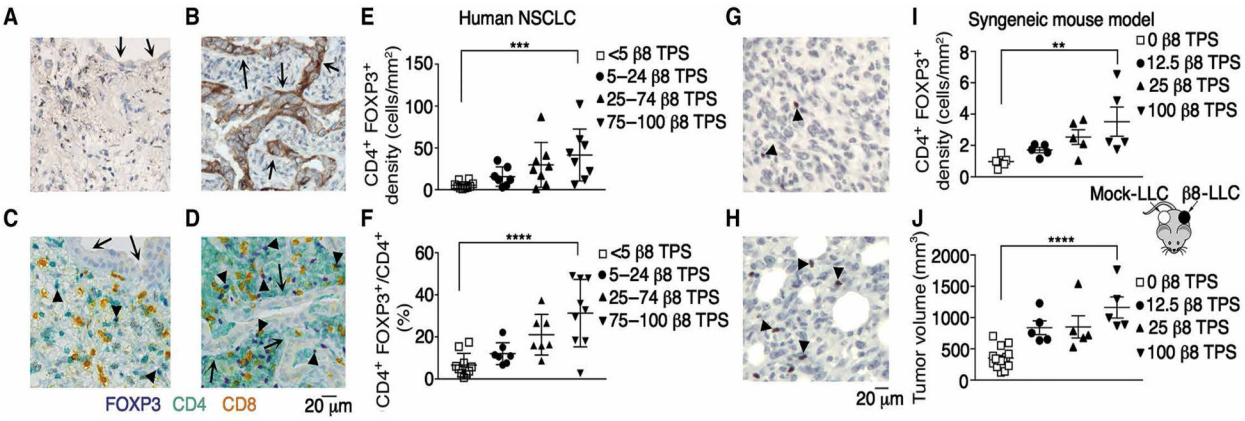

Fig. 6. Proportion of β8-expressing tumor cells correlated with CD4$^+$ FOXP3$^+$ T cell number in human and murine lung cancer.

Representative images of immunohistochemical staining of human (*n* = 32) (**A** to **D**) or murine (*n* = 30) tumors (**G** and **H**). Immunohistochemical localization of integrin β8 in an independent cohort of human NSCLC with a β8 TPS of (A) <10% compared with (B) a high >50% TPS. Arrows in (B) indicate positively staining tumor cells. (C and D) Multiplex immunohistochemical staining of the same samples shown in (A and B) with anti-CD4 (teal), anti-CD8 (yellow), and anti-FOXP3 (purple). Arrows indicate tumor cells, and arrowheads indicate CD4$^+$FOXP3$^+$ cells. Scale bar, 20 μm. (**E**) CD4$^+$FOXP3$^+$ density according to TPS cutoffs <5%, 5 to 24%, 25 to 74%, and 75 to 100%. (**F**) Ratio of CD4$^+$FOXP3$^+$ to all CD4$^+$ cells grouped according to the same cutoffs as in (E) (*n* = 36). (G and H) Immunohistochemical localization of FOXP3$^+$ cells in (G) mock-LLC compared with (H) β8-LLC tumors. Arrowheads point to examples of stained nuclei. Scale bar, 20 μm. (**I**) T_{reg} density depends on proportion of β8-expressing tumor cells. β8-LLC cells were mixed with mock-LLC cells in proportions of 1:0 (filled inverted triangles), 1:4 (filled upright triangles), and 1:8 (filled circles) and injected on the left flanks of mice. Mock-LLC (open squares) was injected on the right flank (see cartoon schematic). Shown are T_{reg} (I) surface density (in mm^2) and (**J**) tumor volume (in mm^3) in mock-LLC tumors compared with tumors with various ratios of β8-LLC to mock-LLC. For multiple comparisons, one-way ANOVA and *P* test for trend were used. ** $P < 0.01$, *** $P < 0.001$, and **** $P < 0.0001$.

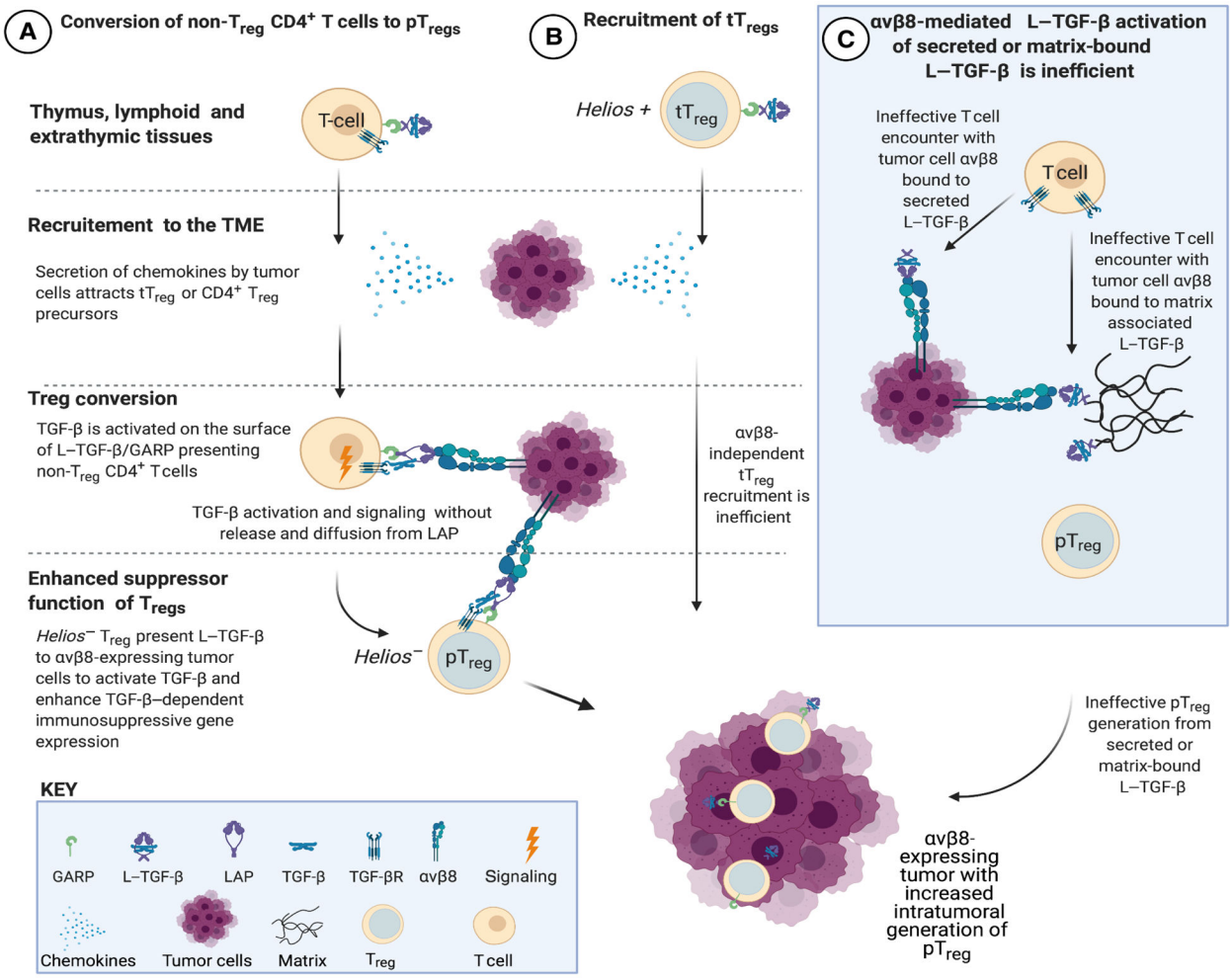

Fig. 7. Proposed mechanisms of T_{reg} enrichment and differentiation in αvβ8-expressing tumors.

(**A**) Non-T_{reg} $CD4^+$ T cells expressing L–TGF-β/GARP infiltrate tumors in response to chemokines in the TME (21). TGF-β cannot interact with TGF-βR unless it undergoes activation. L–TGF-β/GARP–expressing non-T_{reg} $CD4^+$ T cells undergo T_{reg} conversion to $Helios^-$ pT_{reg} after binding to integrin αvβ8 expressed by tumor cells. The mechanism of TGF-β activation does not require the release and diffusion of TGF-β, ensuring that only T cells in contact with αvβ8-expressing tumor cells are converted to pT_{reg} (29). (**B**) Thymically derived $Helios^+$ T_{reg} (tT_{reg}) can potentially be recruited to the TME, but this is not evident in αvβ8-expressing tumors. (**C**) When L–TGF-β is soluble or matrix bound, TGF-βRs are not positioned on the same surface as L–TGF-β. Thus, if active TGF-β is not released from L–TGF-β when exposed to αvβ8 bearing tumor cells, then TGF-βR–expressing T cells need to find, orient, and overcome steric hindrance to bind to TGF-β exposed within the L–TGF-β complex. This activation process is less efficient than when L–TGF-β and TGF-βRs are on the same surface (29). Therefore, soluble or matrix-bound L–TGF-β is less likely to significantly contribute to αvβ8-mediated pT_{reg} conversion in the TME. Created in BioRender.